The development and optimization of techniques for monitoring water quality on-board spacecraft using colorimetric solid-phase extraction (C-SPE)

by

April Ann Hill

A dissertation submitted to the graduate faculty

in partial fulfillment of the requirements for the degree of

DOCTOR OF PHILOSOPHY

Major: Analytical Chemistry

Program of Study Committee:
Marc D. Porter, Co-major Professor
Patricia A. Thiel, Co-major Professor
Robert S. Houk
Theresa L. Windus
David A. Laird

Iowa State University

Ames, Iowa

2007

TABLE OF CONTENTS

ACKNOWLEDGEMENTS

First, I would like to thank my advisor, Marc Porter, for showing me how exciting scientific research can be and for giving me the opportunity to experience 493 amazing parabolas aboard the Vomit Comet. It has truly been a privilege to be a part of the Porter Research Group. I am also sincerely grateful to my co-advisor, Pat Thiel, for supporting my interest in forensic science and for all of her efforts during my last year at ISU.

I would like to express my gratitude to every single member of the Porter Research Group for their openness, kindness, and willingness to help with any problem in or out of the lab. Most importantly, I thank Bob Lipert, my zero-g cohort, for teaching me so much about science and life in general. Thanks also to Cherry Shih, who is the best lab partner, travel companion, bargain shopper and friend anyone could ask for; I am truly lucky to know her. To Sebastian Donner and Jill Uhlenkamp I extend my sincere gratitude for keeping me sane during my last few weeks as a graduate student. To anyone who was ever a part of the Friday lunch group, I miss our fantastic conversations. I am truly grateful to Gufeng Wang for being such a patient teacher and to Becky Staedtler for having all the answers and for always encouraging me.

Finally, I would like to thank my family. To my husband, Randall, who has taught me to take a deeper look at everything, and a deep breath now and then, you have truly made me a better person. I am so happy that your vocabulary skills and my total lack of talent for pool brought us together. To my parents, Tom and Lannie

Bosveld, who I firmly believe are two of the best parents in the world, I cannot express enough gratitude. Thank you, Dad, for believing I could do this since before I could read. And thanks, Mom, for always reminding me that there is more to life than good grades. I am truly lucky to have you both. And last but not least, I thank my grandmother, Ann Bosveld, for so many things I could not possibly list them all.

This work was performed at Ames Laboratory under Contract No. DE-AC02-07CH11358 with the U.S. Department of Energy. This work was supported by NASA (Contract No. NAG91510), DARPA-CEROS, NIH, and by the Institute for Combinatorial Discovery of Iowa State University. The United States Government has assigned the DOE report number IS-T 2890 to this thesis.

GENERAL INTRODUCTION

Dissertation Organization

The main focus of this dissertation is the design, development, and ground and microgravity validation of methods for monitoring drinking water quality on-board NASA spacecraft using colorimetric-solid phase extraction (C-SPE). The Introduction will overview the need for in-flight water quality analysis and will detail some of the challenges associated with operations in the absence of gravity. The ability of C-SPE methods to meet these challenges will then be discussed, followed by a literature review on existing applications of C-SPE and similar techniques. Finally, a brief discussion of diffuse reflectance spectroscopy theory, which provides a means for analyte identification and quantification in C-SPE analyses, is presented.

Following the Introduction, four research chapters are presented as separate manuscripts. Chapter 1 reports the results from microgravity testing of existing C-SPE methods and procedures aboard NASA's C-9 microgravity simulator. Chapter 2 discusses the development of a C-SPE method for determining the total concentration of biocidal silver (i.e., in both dissolved and colloidal forms) in water samples. Chapter 3 presents the first application of our C-SPE technique to the determination of an organic analyte (i.e., formaldehyde). Chapter 4, which is a departure from the main focus of the thesis, details the results of an investigation into the effect of substrate rotation on the kinetics involved in the antigen and labeling steps in sandwich immunoassays. These research chapters are followed by general conclusions and a prospectus section.

NASA Water Quality Monitoring Needs

The current method of monitoring spacecraft drinking water supplies depends on samples collected on the International Space Station (ISS) and returned to Earth for analysis. This process can lead to a gap of several months between sample collection and analysis, which not only introduces the possibility of sample degradation, but also prevents the timely implementation of correction scenarios. These factors underscore the need for rapid, on-board methods for monitoring trace levels of critical components in spacecraft drinking water supplies. However, existent techniques for water quality analysis fail to meet all of the stringent requirements for spaceflight deployment. On-board usage requires methods that provide sufficient selectivity and sensitivity to detect analytes at low concentrations. Flight deployment also requires that the instrumentation be user-friendly, small, lightweight, and capable of operation in microgravity. The preferred methods for water quality testing in most laboratory applications, such as ICP-MS, GC-MS, AA, UV-Vis, etc., require relatively large instrumentation and/or heat sources that are potentially hazardous for use on-board spacecraft. In addition, there are serious concerns related to material toxicity. In answer to this problem, we have developed a technique called colorimetric solid-phase extraction (C-SPE), which has clearly demonstrated an ability to meet the requirements for spacecraft deployment.[1-9] In fact, NASA plans to launch C-SPE in 2009 for a six-month technology demonstration aboard ISS.

Colorimetric Solid-Phase Extraction

C-SPE is a spectrophotometric technique that determines the concentration of an analyte by measuring the change in diffuse reflectance of indicator disks following exposure to a water sample. A hand-held diffuse reflectance (DR) spectrophotometer, shown in Figure 1, is used to rapidly quantify membrane-bound analytes using the Kubelka-Munk (KM) function.[10,11] The complete procedure typically requires only 1-2 min. The instrument, a BYK-Gardner color-guide sphere DR spectrophotometer (Model LCB-6830), is small (8.1 x 17.8 x 9.4 cm), lightweight (0.5 kg), and battery-operated (4 AA), making it attractive for spacecraft deployment in terms of size and power requirements. Other notable features of this instrument include its six-month calibration cycle and long battery life; it can collect 10,000 spectra on a single set of batteries. The instrument is also very user-friendly and can acquire reflectance data in under 2 s over the visible spectral range (400-700 nm) at 20-nm intervals.[6]

Importantly, as the results from recent microgravity testing prove, C-SPE techniques are capable of operation in microgravity. As detailed in Chapter 1, the results of C-SPE analyses for both silver(I) and iodine carried out in microgravity conditions showed excellent agreement with analyses performed in the laboratory. These results prove not only that the chemistries involved in C-SPE analyses are unaffected by reduced gravity, but also that the sample collection procedures are capable of reproducibly metering a target volume of liquid through an SPE disk. The ability to collect a target volume of liquid has long been a challenge for spaceflight

applications because water samples are dispensed from ports using a pressurized system that introduces air bubbles. In microgravity, these air bubbles tend to be finely dispersed, as shown in the photograph in Figure 2, and are therefore difficult to remove.

Another advantage for spacecraft deployment stems from the fact that all C-SPE methods are designed intentionally to use non-hazardous reagents that are either impregnated in the membranes before deployment, or are immobilized on inert media (i.e., glass fiber filters, filter paper, etc.) and introduced into the sample during the analysis. This strategy minimizes the risk of a chemical contamination on-board the spacecraft. It is important to note that the aforementioned characteristics of the C-SPE technique are highly advantageous for a number of Earth-bound applications as well.

There are three main variations of C-SPE: (1) colorimetric complexation followed by product extraction; (2) analyte extraction followed by complexation; and (3) impregnation of colorimetric reagent followed by simultaneous extraction and complexation of the analyte. To date, our laboratory has utilized two of these approaches to develop methods that meet NASA water quality monitoring requirements. Impregnation followed by extraction is the basis of the C-SPE techniques for quantifying the biocidal agents silver(I) and I_2 as well as the metal contaminants copper(II), iron(III), and chromium(VI).[1,2,4,12-14] Complexation and extraction involves colorimetric reagents that are immobilized on inert media and released into samples to form a product that is subsequently collected on an

extraction disk. This technique was demonstrated in the determination of nickel(II).[1,13] Immobilized reagents have also been employed to adjust sample pH and to oxidize an analyte to a more readily detectable product.[1,4] As previously stated, this approach enables C-SPE to function in a "reagentless" format, thereby minimizing exposure to hazardous materials.

The next sections describe the components of C-SPE, including colorimetric chemistry, solid-phase extraction, and DR spectroscopy, illustrating how each contributes to the effectiveness and versatility of C-SPE as an analytical tool.

Colorimetric Reagents

Since many chemicals can form colored compounds, color can be considered a significant analytical tool.[15] Currently, there are standard colorimetric methods for detecting most of the elements, as well as some capable of detecting oxidation states of inorganic compounds, functional groups on organic compounds, etc.[16,17] As such, the use of colorimetric reagents makes C-SPE an extremely versatile technique. The challenge, however, lies in adapting the existing colorimetric methods to function in the reagentless, nontoxic format that makes C-SPE amenable to spaceflight. The preferred embodiment of C-SPE is therefore that of membrane impregnation followed by simultaneous extraction and colorimetric complexation. This tactic is ideal because an analysis is then as simple as collecting a sample of water in a syringe and passing it through an impregnated disk. However, some complexation reactions are slow or simply fail to proceed on the membrane surface (e.g., if the active sites of the reagent are bound to the membrane). In such cases,

one of the other two categories of C-SPE techniques (i.e., analyte complexation followed by product extraction or analyte extraction followed by complexation) may be needed. Once the best format is determined for a particular analysis, the reaction conditions are carefully optimized to yield a C-SPE method that is capable of determining the analyte within a target concentration range (i.e., that dictated by NASA toxicologists).

Solid Phase Extraction

Collecting the colorimetric products on solid-phase extraction (SPE) membranes often enables C-SPE techniques to achieve the low (sub-ppm) detection levels required by NASA. In traditional SPE, analytes are extracted from liquid samples onto a solid adsorbent and are then eluted from the adsorbent using an appropriate solvent. The volume of the eluent is typically much smaller than that of the original sample, resulting in a concentration factor (CF), defined as follows:[18]

$$CF = V_S/V_E \quad (1)$$

where V_S is the sample volume and V_E is the volume of eluent. In C-SPE methods, a colored product formed from the analyte is retained on the SPE disk, causing the disk to undergo a color change. This color change allows for analyte quantification without elution by simply measuring the change in the optical characteristics of the membrane. With the removal of the elution step, the CF is calculated by simply substituting the volume of the extraction membrane for V_E.

Assuming that the colored compound is distributed evenly throughout the entire volume of the extraction disk, a 1.0-mL sample (the volume used for the analyses of total silver and formaldehyde described in chapters 2 and 3) passed through a 13-mm diameter C-SPE membrane would provide a CF of ~150. Earlier data collected in our laboratory suggests that values of CF may be close to 1000.[14] Measuring the color change directly on the solid-phase extraction membrane allows C-SPE techniques to achieve sub-ppm levels of detection using small sample volumes, which is particularly attractive because of the limited water supply in spaceflight.

Diffuse Reflectance Spectroscopy

Quantification of the analytes in C-SPE is accomplished via diffuse reflectance (DR) spectroscopy. When an incident beam is reflected from a rough surface, the reflected radiation consists of two main components: specular reflection and diffuse reflection.[11] Specular reflection results when the beam is reflected from the surface of the sample. If the sample is smooth, the angle of reflection will be equal to the angle of incidence. If the sample is rough, the beam will be reflected at varying angles depending on the orientation (relative to the surface normal) of the particle from which it is reflected.

On the other hand, for samples with rough, non-glossy surfaces (such as the extraction disks used in C-SPE analyses), some of the incident radiation will penetrate into the sample, where it undergoes a combination of scattering (i.e., reflection, refraction, and diffraction) and absorption within the sample.[11] As a result

of these interactions, some of the radiation is redirected toward the surface of the sample, where it exits in all directions with equal intensity, and the surface appears uniformly light at all angles of incidence. This type of reflected radiation, called Kubelka-Munk (KM) reflectance, contains much more information about the sample as a result of the high degree of interaction. This KM reflection is used in much the same way as a UV-Vis absorption spectrum; i.e., to create a reflectance spectrum which contains information about sample composition.

The theory used most often to interpret DR spectra is the KM theory,[10,11] which is an empirical model that allows for quantification of analyte concentrations only if care is taken to ensure that all the assumptions in the theory are met. The assumptions are: (1) there is no specular reflection, (2) the particles within the sample are much smaller than the sample thickness, (3) the sample thickness is greater than the beam penetration depth, and (4) the sample diameter is much greater than the incident beam focus.[11] In C-SPE experiments, Assumptions 2 and 3 are satisfied by the membranes used in the analysis, which consist of poly(styrenedivinylbenzene) particles (~16 μm) embedded in a matrix of polytetrafluoroethylene (PTFE) fibers. The non-glossy surface of the membranes and the design of the instrument work to satisfy Assumption 1 by minimizing, though likely not completely eliminating, specular reflection. Finally, Assumption 4 is maintained by the use of a sample locator/positioner, which ensures that the 11-mm aperture of the instrument is correctly and reproducibly aligned with the exposure area of the C-SPE disks.

In KM theory, the reflectance of a sample is defined as the ratio of the intensities of the reflected and incident radiation. However, it is not practical to measure the absolute reflectance of a sample, so typical DR instruments measure sample reflectance relative to a standard white. This relative reflectance is linearly related to the analyte concentration by the KM function, much like Beer's law relates absorbance to concentration. The KM function is given by equation 2,

$$F(R) = (1 - R)^2 / 2R \qquad (2)$$

where R is the relative diffuse reflectance of the sample. Since the KM reflectance includes contributions from both scattering and absorbance events within the sample, $F(R)$ can be directly related to the concentration of the complex in the membrane, c, by inserting these constants into equation 2 to yield equation 3,

$$F(R) = 2.303\varepsilon c / s \qquad (3)$$

where ε is the molar absorptivity of the colorimetric product and s is the scattering coefficient of the sample surface. The solution concentration of the analyte is determined by means of a calibration plot of $F(R)$ at a given wavelength versus analyte concentration. A complete derivation of the KM theory and a more detailed description of diffuse reflectance spectroscopy can be found in the manuscripts of Blitz, Kortum, and Wendlandt and Hecht.[10,11,19]

Literature Review

As previously mentioned, our laboratory has developed C-SPE methods for the determination of several analytes of interest for water quality monitoring applications. Similar technologies have been developed by other research groups, all of which fall into one of the C-SPE formats previously mentioned: (1) colorimetric complexation followed by product extraction; (2) analyte extraction followed by complexation; and (3) impregnation of colorimetric reagent followed by simultaneous extraction and complexation of the analyte.

In the first variant of C-SPE, complexation followed by extraction, colorimetric reagents are added directly to the sample solution, where the colorimetric reaction takes place. The colorimetric product is then extracted and quantified by DR spectroscopy. This technique is the basis for a procedure in which mercury(II) is determined by complexation with dithizone and extraction onto polystyrene beads.[20] A determination of aluminum in the presence of beryllium was developed using Eriochrome cyanine R (ECR) and cellulose, where the beryllium/ECR complex is not sorbed by cellulose.[21] Nickel can be determined by reacting with dimethylglyoxime (DMG) or benzyldioxime (BD) and retaining the complex on either silica gel or microcrystalline cellulose.[22,23] In another study, Co(II), Ni(II), Fe(II) and Fe(III) were complexed with nitroso-R-salt (NRS) and concentrated on membrane filters for DR spectroscopic analysis.[24] The noble metals have been determined using their complexes with azorhodanines, tyrodine, and sulfonitrophenol M.[25] Vanadium has also been quantified using sulfonitrophenol M.[26] Octadecyl silica has been used to

extract trace levels of nitrite in water following complexation with Shinn reagent,[27] and low concentrations of molybdenum(VI) have been detected on silica gel after complexation with bromopyrogallol red in the presence of cetylpyridinium bromide (a cationic surfactant).[28]

The second embodiment of C-SPE (extraction followed by colorimetric complexation), usually involves solid sorbents that have been impregnated with ion exchange media. The analytes (i.e., aqueous anions and cations) are adsorbed by the ion exchange media, which are then exposed to the colorimetric reagent. This technique has been employed to quantify mixtures of vanadium and molybdenum using 8-hydroxyquinoline-5-sulfonic acid and phenylfluorone,[29] rhenium with thiocyanate,[30] and lead with 4-(2-pyridylazo)resorcinol (PAR).[31,32] After complexing with chloride, Hg(II) was detected by extraction onto an anion exchange resin and exposure to dithizone.[33-35] Arsenic(V) has been extracted onto an anion exchanger and detected as a molybdoarsenic heteropoly acid.[36] Copper(II), chromium(VI) and nickel(II) were detected simultaneously by extracting onto two different fibrous disks and reacting with three different colorimetric reagents.[37] In this method, an anion exchange disk adsorbed Cr(VI), where it was reacted with 1 ,5-diphenylcarazide, while the nickel and copper were extracted onto a cation exchange disk and exposed to sodium diethyldithiocarbamate (for Cu(II) detection) and DMG (for Ni(II) detection).

The third C-SPE variant, impregnation of a colorimetric reagent followed by extraction of the analyte, has been used for the separate, simultaneous

determination of cobalt(III) and palladium(II), copper(II) and zinc(II) using 4-(2-thiazolylazo)resorcinol (TAR) immobilized on silica gel.[38,39] Similar studies investigated the determination of transition metals with 1-(2-pyridylazo)-2-naphthol (PAN)[40,41] and of indium and lead using PAR. [31,42] Heterocyclic azo compounds immobilized on silica gel have been used for the simultaneous determination of cobalt and palladium.[39] Thorium has been detected using arsenazo I,[43] nickel with benzylglyoxime and DMG,[44] and zinc using immobilized 1,10-phenanthroline in the presence of bromophenol blue.[45] Lead and zinc have been detected using silica-immobilized Xylenol Orange,[46] and iron using bathophenanthroline.[47] Bismuth(III) and copper(II) have been determined using sorbents prepared by immobilizing bismuthol I on silica gel and natural zeolite, respectively.[48,49] An indirect determination of fluoride has been developed using the decrease in color of immobilized thorium complexes of Arsenazo I upon exposure to flouride.[50] Given this extensive list of analytes that have been detected using various embodiments of C-SPE, this technology has proven to be a powerful analytical tool with the potential for widespread usage.

Dissertation Overview

This thesis is primarily focused on the application of the techniques and concepts outlined above to the development and validation of C-SPE methods for monitoring drinking water quality on-board NASA spacecraft. The following three research chapters, presented as separate manuscripts, detail the development and microgravity evaluation of C-SPE methods designed to address the specific

concerns for water quality monitoring in space exploration. Chapter 1 presents the results of testing aboard NASA's C-9 microgravity simulator, where the spaceflight compatibility of existing C-SPE methods, including chemistries and sample handling techniques, was verified. Chapter 2 discusses the development of a C-SPE method capable of determining both dissolved and colloidal forms of silver, which serves as a biocide in spacecraft water samples. Chapter 3 reports on the first C-SPE method developed in our laboratory for the determination of an organic analyte (i.e., formaldehyde). Chapter 4, the final research chapter, is a departure from the main topic of the thesis. This chapter presents a detailed investigation of the use of substrate rotation to reduce the time required for performing sandwich immunoassays. The dissertation closes with a discussion of the general conclusions as well as a future prospectus.

References

(1) Arena, M. P.; Porter, M. D.; Fritz, J. S. *Anal. Chem.* **2002**, *74*, 185-190.

(2) Arena, M. P.; Porter, M. D.; Fritz, J. S. *Anal. Chim. Acta* **2003**, *482*, 197-207.

(3) Arena, M. P.; Porter, M. D.; Fritz, J. S.; Mudgett, P.; Rutz, J.; Schultz, J. *32nd International Conference on Environmental Systems, San Antonio, TX* **2002**, *SAE Technical Paper #2002-01-2535.*

(4) Gazda, D. B.; Fritz, J. S.; Porter, M. D. *Anal. Chim. Acta* **2004**, *508*, 53-59.

(5) Gazda, D. B.; Fritz, J. S.; Porter, M. D. *Anal. Chem.* **2004**, *76*, 4881-4887.

(6) Gazda, D. B.; Lipert, R. J.; Fritz, J. S.; Porter, M. D.; Rutz, J.; Mudgett, P.; Schultz, J. *33rd International Conference on Environmental Systems, Vancouver, B.C., Canada* **2003**, *SAE Technical Paper #2003-01-2406*.

(7) Porter, M.; Arena, M.; Weisshaar, D.; Mudgett, P.; Rutz, J.; Benoit, M.; Colorimetric Solid Phase Extraction Measurements of Spacecraft Drinking Water Contaminants in: *KC-135 Postflight Report*, 2004.

(8) Porter, M. D.; McCoy, J. T.; Hazen-Bosveld, A. A.; Lipert, R. J.; Nordling, J.; Shih, C. J.; Gazda, D. B.; Rutz, J.; Straub, J.; Schultz, J.; Alverson, J.; Colorimetric Solid Phase Extraction Measurements of Spacecraft Drinking Water Contaminants in: *C-9 Postflight Report*, 2006.

(9) Dias, N. C.; Porter, M. D.; Fritz, J. S. *Anal. Chim. Acta* **2006**, *558*, 230-236.

(10) Kortum, G. *Reflectance Spectroscopy: Principles, Methods, Applications*; Springer: New York, 1969.

(11) Blitz, J. P. In *Modern Techniques in Applied Molecular Spectroscopy*; Mirabella, F. M., Ed.; John Wiley and Sons, Inc.: New York, 1998, pp 185-217.

(12) Fritz, J. S.; Arena, M. P.; Steiner, S. A.; Porter, M. D. *J Chromatogr. A* **2003**, *997*, 41-50.

(13) Gazda, D. B.; Lipert, R. J.; Fritz, J. S.; Porter, M. D. *Anal. Chim. Acta* **2004**, *510*, 241-247.

(14) Fritz, J. S.; Arena, M. P.; Steiner, S. A.; Porter, M. D. *J Chromatogr. A* **2003**, *997*, 41-50.

(15) Bartecki, A.; Burgess, J. *The Colour of Metal Compounds*; Gordon and Breach: Amsterdam, 2000.

(16) Thomas, L. C.; Chamberlin, G. J. *Colorimetric Chemical Analysis Methods*, 9th ed.; John Wiley and Sons: New York, 1980.

(17) Marczenko, Z. *Separation and Spectrophotometric Determination of Elements*, 2nd ed.; Ellis Horwood: Chichester, 1986.

(18) Fritz, J. S. *Analytical Solid-Phase Extraction*; John Wiley & Sons: New York, 1999.

(19) Wendlandt, W. W.; Hecht, H. G. *Reflectance Spectroscopy*; John Wiley & Sons: New York, 1966.

(20) Paradkar, R. P.; Williams, R. R. *Appl. Spectrosc.* **1996**, *50*, 753-758.

(21) Ershova, N. I.; Ivanov, V. M. *Anal. Chim. Acta* **2000**, *408*, 145-151.

(22) Ivanov, V. M.; Ershova, N. I. *Vestnik Moskovskogo Universiteta, Seriya 2: Khimiya* **1999**, *40*, 22-26.

(23) Ershova, N. I.; Ivanov, V. M. *Fresenius. J. Anal. Chem.* **1999**, *363*, 641-645.

(24) Yokota, F.; Endo, M.; Abe, S. *Bunseki Kagaku* **1999**, *48*, 1135-1140.

(25) Gur'eva, R. F.; Savvin, S. B. *Zh. Anal. Khim.* **2000**, *55*, 249-254.

(26) Gur'eva, R. F.; Savvin, S. B. *Zh. Anal. Khim.* **2001**, *56*, 901-904.

(27) Miro, M.; Frenzel, W.; Estela, J. M.; Cerda, V. *Analyst (Cambridge, United Kingdom)* **2001**, *126*, 1740-1746.

(28) Ivanov, V. M.; Mamedova, A. M. *Zh. Anal. Khim.* **2006**, *61*, 242-249.

(29) Shvoeva, O. P.; Dedkova, V. P.; Savvin, S. B. *Zh. Anal. Khim.* **2000**, *55*, 545-548.

(30) Borisova, L. V.; Gatinskaya, N. G.; Savvin, S. B.; Ryabukhin, V. A. *Zh. Anal. Khim.* **2002**, *57*, 134-137.

(31) Shvoeva, O. P.; Dedkova, V. P.; Savvin, S. B. *Zh. Anal. Khim.* **2001**, *56*, 1080-1083.

(32) Shvoeva, O. P.; Dedkova, V. P.; Savvin, S. B. *Zh. Anal. Khim.* **2001**, *56*, 376-379.

(33) Dedkova, V. P.; Shvoeva, O. P.; Savvin, S. B. *Zh. Anal. Khim.* **2004**, *59*, 381-385.

(34) Shvoeva, O. P.; Dedkova, V. P.; Savvin, S. B. *Zh. Anal. Khim.* **2003**, *58*, 528-532.

(35) Shvoeva, O. P.; Dedkova, V. P.; Savvin, S. B. *Zh. Anal. Khim.* **2004**, *59*, 623-627.

(36) Dedkova, V. P.; Shvoeva, O. P.; Savvin, S. B. *Zh. Anal. Khim.* **2002**, *57*, 298-302.

(37) Dedkova, V. P.; Shvoeva, O. P.; Savvin, S. B. *Zh. Anal. Khim.* **2001**, *56*, 758-762.

(38) Ivanov, V. M.; Kuznetsova, O. V. *Zh. Anal. Khim.* **2000**, *55*, 899-903.

(39) Ivanov, V. M.; Kuznetsova, O. V.; Grineva, O. V. *Zh. Anal. Khim.* **1999**, *54*, 233-236.

(40) Ivanov, V. M.; Morozko, S. A.; Kachin, S. V. *Zh. Anal. Khim.* **1994**, *49*, 857-861.

(41) Morozko, S. A.; Ivanov, V. M. *Zh. Anal. Khim.* **1995**, *50*, 572-578.

(42) Ivanov, V. M.; Ershova, N. I. *Vestnik Moskovskogo Universiteta, Seriya 2: Khimiya* **1998**, *39*, 101-103.

(43) Ivanov, V. M.; Ershova, N. I.; Figurovskaya, V. N. *Zh. Anal. Khim.* **2003**, *58*, 318-321.

(44) Ershova, N. I.; Ivanov, V. M. *Fresenius. J. Anal. Chem.* **2000**, *367*, 210-211.

(45) Zaporozhets, O. A.; Ivan'ko, L. S.; Bykova, L. V.; Mostovaya, N. A. *Zh. Anal. Khim.* **2004**, *59*, 23-27.

(46) Zaporozhets, O. A.; Tsyukalo, L. E. *Zh. Anal. Khim.* **2004**, *59*, 386-391.

(47) Saito, T. *J. AOAC Int.* **1994**, *77*, 1031-1035.

(48) Ivanov, V. M.; Polyanskov, R. A. *Vestnik Moskovskogo Universiteta, Seriya 2: Khimiya* **2006**, *47*, 402-408.

(49) Ivanov, V. M.; Polyanskov, R. A.; Sedova, A. A. *Vestnik Moskovskogo Universiteta, Seriya 2: Khimiya* **2005**, *46*, 61-65.

(50) Ivanov, V. M.; Ershova, N. I.; Figurovskaya, V. N. *Zh. Anal. Khim.* **2004**, *59*, 314-318.

Figure 1. BYK-Gardner color-guide sphere DR spectrophotometer (8.1 x 17.8 x 9.4 cm).

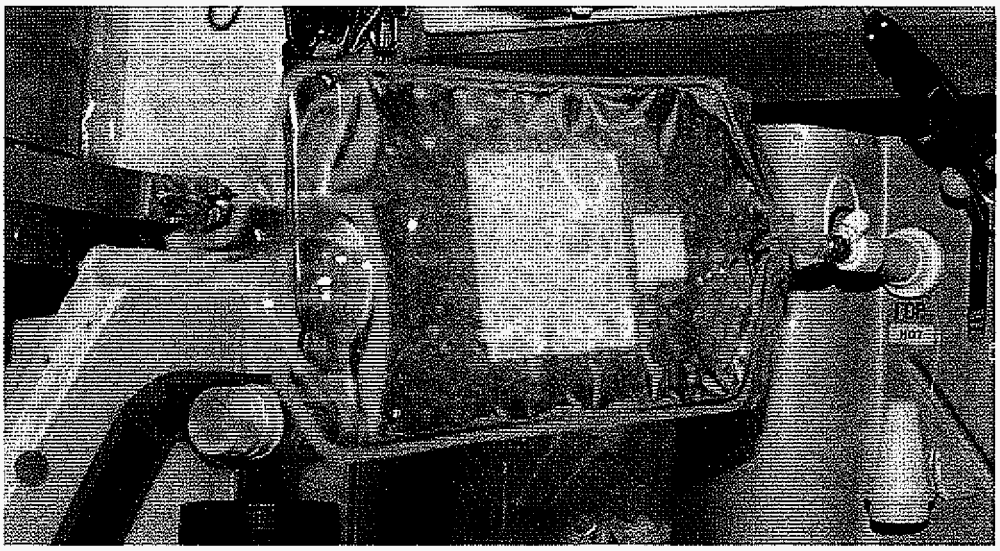

Figure 2. Photograph of typical air-water dispersion in a water sample collection bag on-board ISS.

CHAPTER 1. COLORIMETRIC-SOLID PHASE EXTRACTION TECHNOLOGY FOR WATER QUALITY MONITORING: EVALUATION OF C-SPE AND DEBUBBLING METHODS IN MICROGRAVITY

April A. Hazen-Bosveld, Robert J. Lipert, John Nordling, Chien-Ju Shih
Iowa State University, Ames, IA 50011

Marc D. Porter, Lorraine M. Siperko
Arizona State University, Tempe, AZ 85287

Daniel B. Gazda, Jeff A. Rutz, John E. Straub, John R. Schultz
Wyle Laboratories, Houston, TX 77058

J. Torin McCoy
NASA, Johnson Space Center, Houston, TX 77058

Abstract

Colorimetric-solid phase extraction (C-SPE) is being developed as a method for in-flight monitoring of spacecraft water quality. C-SPE is based on measuring the change in the diffuse reflectance spectrum of indicator disks following exposure to a water sample. Previous microgravity testing has shown that air bubbles suspended in water samples can cause uncertainty in the volume of liquid passed through the disks, leading to errors in the determination of water quality parameter concentrations. We report here the results of a recent series of C-9 microgravity experiments designed to evaluate manual manipulation as a means to collect bubble-free water samples of specified volumes from water sample bags containing up to 47% air. The effectiveness of manual manipulation was verified by comparing the results from C-SPE analyses of silver(I) and iodine performed in-flight using samples collected and debubbled in microgravity to those performed on-ground

using bubble-free samples. The ground and flight results showed excellent agreement, demonstrating that manual manipulation is an effective means for collecting bubble-free water samples in microgravity.

1. Introduction

A critical aspect of spacecraft crew health assurance is maintaining a safe supply of drinking water. To this end, this project is focused on the development and deployment of chemical sensor methodologies for water quality monitoring in the life support systems used for space exploration. Among the key constituents in spacecraft drinking water are iodine and silver; the biocides used in the U.S. and Russian ISS potable water systems, respectively. The water monitoring methods under development for these biocides are based on an innovative solid phase extraction (SPE)[1] technique called colorimetric-SPE (C-SPE).[2-11] This paper presents recent progress in the development of rapid, simple, and reliable C-SPE methods that mitigate the potential detrimental effects of air bubbles present in water samples collected in microgravity.

C-SPE is a spectrophotometric technique based on measuring the change in diffuse reflectance of indicator disks following exposure to a water sample. A hand-held diffuse reflectance spectrophotometer is used to quantify membrane-bound analytes using the Kubelka-Munk function.[12-14] The Kubelka-Munk function relates the diffuse reflectance of an opaque sample to its absorption coefficient k, and scattering coefficient s as given by the following equation:

$$F(R) = \frac{(1-R)^2}{2R} = \frac{k}{s} \quad (1)$$

where *F(R)* is the Kubelka-Munk function and *R* is the relative reflectance of the sample (i.e., reflectance measured relative to a nonabsorbing standard). When measuring the reflectance of an absorbing species diluted in a nonabsorbing matrix relative to the reflectance of the pure matrix, the absorption coefficient *k* may be replaced by the product $2.303\varepsilon C$, where ε is the extinction coefficient and *C* is the molar concentration. Then

$$F(R) = \frac{2.303\varepsilon}{s} C . \quad (2)$$

To determine analyte concentrations, spectra were transformed to obtain the value of the Kubelka-Munk function at the appropriate analytical wavelength. This value is then used to quantify the analyte via a standard response curve.

Quantitative measurement of analyte concentrations requires the metering of a known volume of water through a C-SPE indicator disk. Air bubbles suspended in water samples in microgravity can cause uncertainty in the volume of liquid passed through the disks, leading to errors in concentration determinations. To address this issue, a series of C-9 microgravity experiments were recently conducted with the following goals: 1) develop procedures for manual manipulation of water sample bags to separate air/water mixtures, thus enabling the collection of bubble-free 1-mL and 10-mL water samples in microgravity; 2) verify the functionality of C-SPE test methods in microgravity by demonstrating analyses for the biocides silver(I) and iodine using aqueous samples consisting of dispersed air/water mixtures containing

up to 50% air; and 3) determine whether bubble-free samples containing the expected amount of reagent can be collected when utilizing the reagent introduction procedure required during the syringe-filling step for the C-SPE analyses of both total iodine and total silver, which are to be evaluated on a future set of C-9 flights. To achieve these goals, experiments were conducted on four C-9 flights as described below.

Flight 1: Manual bubble mitigation and syringe filling

Evaluate manual bubble mitigation strategies for the 30-mL water sample collection bags used for silver(I) analysis and the 155-mL bags used for iodine analysis.

Determine procedures for filling syringes with either 10.0 mL of bubble-free iodine water or 1.0 mL of bubble-free silver water from sample collection bags containing a dispersed 50/50 air/water mixture.

Evaluate the performance of bubble removal strategies by comparing the mass of liquid in 1-mL and 10-mL syringes filled in flight from sample collection bags with up to 50% air to that of the same syringes filled on the ground from bubble-free collection bags.

Flight 2: Silver(I) analysis

Demonstrate agreement between ground and flight data from silver(I) C-SPE analyses of samples containing up to 50% air.

Flight 3: Iodine analysis

Demonstrate agreement between ground and flight data from iodine C-SPE analyses with samples that contain up to 50% air.

Flight 4: Evaluation of reagent introduction procedures

Determine the amount of reagent drawn into a syringe from a reagent cartridge present in line between the sample collection bag and syringe.

Determine the volume of air drawn into the syringe (i.e., the effective dead volume of the reagent cartridge) and the volume of liquid drawn into the syringe when the plunger of the syringe is withdrawn to a prespecified mark.

Evaluate procedures for removal of air from syringes filled by drawing liquid through an in-line reagent cartridge.

2. Materials and Methods

Instrumentation

Both in-flight and ground-based C-SPE measurements were made using BYK Gardner Color Guide spin d/8° diffuse reflectance spectrophotometers. All mass measurements were performed using a calibrated Mettler Toledo model AG205 analytical balance.

Silver(I)-sensitive membranes

A solution of 5-[4-(dimethylamino)benzylidene]rhodanine (DMABR) (Aldrich) was prepared by dissolving 0.1523 g DMABR in 50 mL of dimethyl formamide in a 250-mL volumetric flask. Solubilization required sonicating for ~5 min, after which

the solution was brought to volume using methanol. A second solution was prepared by pipetting 3.073 g Brij 30 surfactant (Aldrich) into a tared Nalgene bottle on a balance and bringing the total mass to 100.4 g with deionized water.

These solutions were used to impregnate 3M Empore SDB-XC (polystyrene-divinylbenzene) 47-mm extraction membranes. Each membrane was placed into an all-glass filter holder assembly (Millipore), and 10.0 mL of the DMABR solution were pipetted into the funnel. Next, a vacuum pump was used to apply a pressure differential across the membrane of ~1 inch of Hg to pull the solution through the membrane. After the DMABR solution had passed through the membrane, the pressure differential was maintained for another 10 s to remove residual liquid. The funnel then was separated from the filter holder and wiped clean with a methanol-wetted Kimwipe to remove residual solution, which tends to form DMABR particulates when exposed to water. The cleaned funnel was reattached to the filter holder, and 5.0 mL of the Brij 30 solution were added via a pipette. A vacuum-derived pressure of ~3.5 inches of Hg was applied to pull this solution through the membrane. This pressure differential was subsequently increased to ~20 inches of Hg (the maximum attainable pressure differential) for 30 s to dry the membrane. After reagent impregnation, the membranes were allowed to dry further by storage for ~12 h in a closed drawer before being cut into 13-mm disks using a cork borer.

Iodine-sensitive membranes

A solution was prepared by dissolving 3.0112 g poly(vinylpyrrolidone) (PVP: MW = 10,000) (Sigma-Aldrich) in 50 mL of 1:1 methanol:water in a 100-mL

volumetric flask. This solution was then brought to volume with 1:1 methanol:water. Iodine-sensitive membranes were prepared by passing 10.0 mL of this solution through an Empore SDB-XC membrane using the aforementioned vacuum filtration system. A pressure difference of ~3.5 inches of Hg was required to drive this solution through the membrane. Once the solution had passed, the pressure difference was maximized for 45 s to remove residual solvent and dry the membrane. These membranes were also stored for ~12 h in a dark drawer before being cut into 13-mm disks.

NaCl-loaded glass wool and paper disks

Sodium chloride (NaCl) was used as a simulant for the introduction of reagent into water samples. Two different types of reagent disks were prepared. The first type, designed to simulate the Oxone-coated glass wool used in the analysis of total iodine,[9] was prepared by evaporating an aqueous solution of NaCl onto glass wool. A sheet of glass wool was cut to fit into a 140-mm diameter Petri dish, and ~20-mL of a solution containing 4.00 g NaCl in water was poured over it. The glass wool was then dried in a 105 °C oven for ~2 h. The dried glass wool was subsequently cut into 13-mm diameter disks, each containing ~34.5 mg NaCl.

The second type of NaCl disk was prepared from filter paper, which is used to introduce the colorimetric reagent in the analyses of formaldehyde [11] and nickel [8] by C-SPE. To prepare this type of disk, 50-µL of a solution containing 10.5 mg/mL NaCl (aq) was pipetted onto a 13-mm diameter disk of Whatman #1 filter paper. The water

was then dried at room temperature for ~12 h, yielding a NaCl-impregnated disk containing 0.5 mg NaCl.

C-SPE cartridges

All C-SPE membranes and NaCl-coated media were prepared the day before their corresponding flight. A few hours prior to flight, the appropriate membranes or media were cut into 13-mm disks and loaded into Swinnex polypropylene filter holders. These filter holders have Luer fittings that readily form leak-tight connections with a syringe and waste collection bag. Additionally, the holders contain a Teflon gasket that defines the area of the membrane disk exposed to the water sample and forms an internal seal within the cartridge.

Silver(I) solutions

Silver solutions were prepared in opaque Teflon bottles by diluting a silver(I) atomic absorption standard (Aldrich) with deionized water. Five solutions were prepared by pipetting a predetermined mass of the standard into a tared Teflon bottle on a balance and bringing the total mass to 100 g. The actual silver concentrations, as determined by ICP-MS, were 0.000, 0.238, 0.478, 0.703, and 1.03 ppm.

Iodine solutions

Five iodine sample solutions were prepared gravimetrically by diluting the appropriate mass of a 100-ppm iodine stock solution (made by diluting a volumetric iodine standard solution (Fixanal, Riedel-de Haen) with deionized water) to 500 g in

a 500-mL opaque Teflon bottle. The actual iodine concentrations were determined by the Leuco Crystal Violet method [15] to be 0.000, 0.106, 0.302, 1.66, and 3.60 ppm.

3. Procedures, Results, and Discussion

All flight experiments were performed aboard NASA's Reduced Gravity Office's C-9 aircraft. Each flight consisted of 4 sets of 10 parabolas (40 total parabolas) that created alternating high gravity and microgravity environments. Efforts were taken to design experiments that could be broken into discrete steps that could be completed in a single microgravity segment.

Flight 1: Manual bubble mitigation and syringe filling

Procedures

Teflon sample bags (American Fluoroseal) were prepared to contain predetermined air-water mixtures. To mimic a silver(I) analysis, 30-mL capacity bags were filled with 15 mL of air and 15 mL of water with two drops of red food coloring to enhance bubble visibility. To mimic an iodine analysis, 155-mL capacity bags were filled with 20 mL of air and 60 mL of water with two drops of blue food coloring. During the microgravity portions of the first 10 parabolas, fliers worked in pairs to test various approaches for manipulating the sample bags (one type of bag per pair) and to practice filling syringes using the method found to be the most effective. For the simulated silver(I) analysis, 1-mL plastic, single-use syringes (Norm-Ject, Henke Sass Wolf) were filled from the 30-mL bags. For iodine, 10.0-mL samples were collected from the 155-mL bags using 10 and 25-mL glass syringes (SGE

International Pty. Ltd.). If bubbles were observed, the syringe was overfilled and swung in an arc to drive bubble-free water to the plunger end of the syringe. The air was then pushed back into the sample bag as the plunger was adjusted to the 10.0-mL mark. During the second set of 10 parabolas, each pair of fliers debubbled bags and filled syringes, which were capped and returned to JSC for ground measurements of the collected water mass. The types of sample bags and syringes were then switched between the pairs of fliers and the process repeated during the second half of the flight.

Each parabola began with dispersion of the air into the water phase, followed by a quick, vigorous fling of the bag in an arc to force liquid into the narrow tube at the exit port. Then, various techniques of swinging the bag in arcs were tested to accumulate a bubble-free volume of liquid at the exit port. These manipulations represent a manual form of centrifugation of the liquid in the bag. Extensions of this general theme included: 1) attachment of plastic clamps to the bags to isolate the liquid from the gas phase after centrifugation; and 2) tests of an aspiration valve that was attached to a waste bag in order to remove the small plug of air introduced by the syringe inlet. All manipulations, from air dispersal through syringe filling, were performed in a single microgravity parabola. Figure 1 presents a photograph from the in-flight filling of a 1-mL syringe from a manually debubbled sample bag.

Results

The accuracy and reproducibility of filling syringes from bags containing up to 50% air are given in Table 1. A total of twenty 1-mL samples were collected in flight,

5 by each flier. For the larger syringes, eight 10-mL and nine 25-mL syringes were successfully filled in flight out of a targeted 10 each. All 10 samples could not be collected because each bag was only ~13% full when the final sample was collected, and obtaining a plug of liquid in bags with such a large void volume was a difficult task to accomplish in a 25-s parabola.

As is evident from Table 1, manual bubble mitigation is very effective for the production of bubble-free water samples, facilitating the accurate and reproducible metering of liquids in microgravity. It is also important to note that these results were obtained with all manipulations performed in a single, ~25 s microgravity period. We firmly believe that even closer agreement with ground data could be obtained on ISS or Shuttle, where the relaxed time constraints will enable even more effective sample manipulation and phase separation.

Discussion

The simplest procedures proved highly effective for the accurate and precise metering of liquids from sample bags containing air/water mixtures. We found that while the aspiration valve assembly would generate bubble-free liquids in the syringes, the same results were obtained without the valve by rapidly pumping a filled syringe that contained a bubble back into the sample collection bag and refilling the syringe. Therefore, aspiration valves were not used to collect samples for the mass determination.

Clamps were also found to be effective in isolating a portion of bubble-free liquid in a section of the sample bag. However, good results were also obtained by

simply making a clamp with your fingers or by bag-folding. These procedures were found to minimize the time required for sample collection, ensuring that the entire process could be completed in the microgravity segment of a single parabola. We acknowledge that each set of experiments employed two fliers to fill a single syringe, which will not be feasible on-orbit. Since we are anticipating that only one astronaut will be available to perform these tasks on ISS or Shuttle, it may be preferable to use clamps to facilitate the withdrawal of samples without re-dispersing air into the liquid phase.

Flight 2: Silver analysis

Procedures

Prior to this flight, 20 mL of each silver(I) solution were loaded into 30-mL sample bags, followed by 15 mL of air. All sample bags, syringes (HSW 1-mL polyethylene syringes), and silver-sensitive membrane cartridges were color-coded for each concentration. Four replicate experiments were carried out at each sample concentration, both in-flight and on the ground. To isolate the effects of microgravity on the analysis, ground and flight experiments were performed concurrently. The ground experiments mimicked both the thermal environment (~14-23 °C) and the time constraints of the aircraft. Notably, as the 1-mL samples were removed from each bag during flight, the liquid/air ratio in each bag decreased from ~57% for filling the first syringe to 53% when filling the last syringe. A typical microgravity flight consists of four sets of ten parabolas. During the first few parabolas of each set, a 1-mL sample was collected from each bag. This task was accomplished by having

one flier manipulate the bag to disperse air, and then manually debubble the sample bag in the manner determined during Flight 1. The same flier then held the bag while the partner flier attached a corresponding, color-coded syringe to the bag and filled it to the 1.0-mL mark. These syringes were capped and stored in a syringe holder firmly mounted to the flight table. With four fliers working in teams of two (Fliers 1 and 2 in Team 1 and Fliers 3 and 4 in Team 2), four syringes were filled in the first two parabolas.

On Parabola 3, the tasks changed. Team 1 stopped filling syringes, and began the analyses of the syringe-loaded samples. Thus, while Team 2 filled the fifth and final syringe for that particular set of ten parabolas, Flier 1 passed one of the 1.0-mL samples through its corresponding, color-coded cartridge. On Parabola 4, Flier 2 dried this membrane by passing 60 mL of air through the cartridge using a syringe. On Parabola 5, Flier 3 opened the cartridge, mounted the bottom section, which contained the membrane, on the sample locator, and measured the spectrum of the disk with the hand-held diffuse reflectance spectrometer while Flier 4 recorded the sample number, cartridge color, and any observations about that sample. This process was repeated until all five samples were analyzed. The entire procedure was repeated for each of the four sets of ten parabolas. The data analysis of these results, which was completed upon returning to JSC, included downloading the spectra to a laptop computer, converting reflectance data using the Kubelka-Munk function, *F(R)*,[13] and plotting *F(R)* versus concentration.

Results

Four samples of each concentration were tested in both the ground and flight experiments. Figure 2 is a plot of all data collected, after Kubelka-Munk workup, in both sets of experiments. Table 2 lists the calibration equation, the correlation coefficient, and the calculated limit of detection (LOD) obtained from each experiment.

Discussion

The agreement between the ground and flight results shown in Figure 2 for the analysis of silver by C-SPE is excellent. These results clearly demonstrate that the entire analysis, from sample collection to data acquisition, can be reliably carried out in microgravity and indicate that the method is viable for on-orbit tests during spaceflight.

Although linear regressions were applied to the data for comparison purposes, a small, reproducible degree of non-linearity exists at the lower concentration range. The origin of this dependence is under investigation. As a consequence, the LOD was calculated by using the response of the blank and the lowest of the silver(I) concentrations tested, 0.238 ppm. Importantly, the ~30 ppb LOD for the in-flight data easily meets NASA's desired monitoring range of 0.1 to 1.0 ppm.

Flight 3: Iodine analysis

Procedures

Prior to flight, five 155-mL, color-coded sample bags were filled with different concentrations of iodine solutions. After preparation, each bag contained 60 mL of iodine solution and 20 mL of air, which enabled the collection of four 10-mL samples from each bag during the flight. Through the course of the flight, the liquid/air ratio in each bag during the debubbling step ranged from 75% for the first sample to 60% for the fourth sample. In all other ways the procedure for this experiment was identical to that used in the silver flight.

Results

The data collected during the ground and flight experiments are plotted in Figure 3, while Table 3 shows a comparison between the ground and flight calibration equations. The limits of detection listed in Table 3 were calculated as described for the silver(I) experiment.

Discussion

As with the silver(I) results, the agreement between the ground and flight data for I_2 is excellent. The slight negative deviation in the data from the flight experiment, while well within the in-flight performance requirements, is attributed to two factors. First, a very small, but not quantifiable level of leakage of the iodine solutions from the cartridges was observed during flight. A loss of solution while metering the liquid through the membrane, would, of course, result in a negative deviation in the response with respect to the ground data. This issue results from the

25 s time limits imposed by C-9 testing, which require forcing the 10-mL liquid sample through the membrane at a high rate. Second, the sample bags used for flight were filled before those used on-ground, thereby exposing the flight solutions to light for a longer period of time. Since iodine solutions are light sensitive, the flight solutions may have degraded slightly more than the ground samples. Despite these concerns, which are of minimal importance given the excellent agreement between ground and flight data, these results indicate that the entire procedure for this analysis can be easily performed in microgravity with an extremely high level of effectiveness.

Flight 4: Evaluation of reagent introduction procedures

Procedures

The results from the first three flights have shown that bubble-free samples ranging from 1.0-mL to 10.0-mL can be collected into syringes from bags containing up to 50% air. However, some of the C-SPE methods being developed for NASA, including those for total iodine, total silver, nickel, and formaldehyde[2,8,9,11] involve the use of a reagent cartridge in line between the sample bag and syringe. The reagent cartridge contains an inert medium, such as glass wool or filter paper, that has been impregnated with, for example, an oxidizing agent, pH buffer, colorimetric reagent, or masking agent, which is then introduced into the solution as it enters the syringe. Because the reagent cartridge also contains an unknown dead volume of air, air enters the syringe even when collecting samples from a debubbled bag.

The methods under development involve filling either a 10-mL glass syringe (e.g., total iodine) or a 3-mL polyethylene syringe (e.g., total silver, nickel, and formaldehyde) through a Swinnex cartridge containing the reagent medium. For this flight experiment, several syringes were filled from debubbled sample bags through C-SPE cartridges containing either NaCl-impregnated glass wool or filter paper disks. The filled syringes were returned to the ground where several performance metrics were determined, including the amount of NaCl dissolved by the liquid sample due to its in-flight passage through the reagent cartridge, and the amount of air introduced into the syringe by the cartridge dead volume.

During the first two sets of parabolas (parabolas 1-20), Fliers 1 and 2 filled 10-mL and 3-mL polyethylene syringes to the mark (3.0 or 10.0-mL) from debubbled sample bags containing deionized water. Five syringes of each volume were filled through NaCl-coated glass wool cartridges and five through NaCl-impregnated filter paper cartridges. Fliers 3 and 4 documented these proceeding with photographs and videos. These syringes were capped and returned to the ground-based laboratory where the amount of liquid collected in each syringe was determined gravimetrically. This value was then used to calculate the cartridge dead volume, while the concentration of Na^+ in each sample was determined by ICP-MS.

During the following parabolas, the four fliers broke into two-member teams to collect and debubble five samples through each type of cartridge. Fliers 1 and 2 collected five separate 10.0-mL samples using 10-mL glass syringes, while Fliers 3 and 4 collected 1.0-mL samples using 3-mL polyethylene syringes. To collect a

sample, the plunger was first pulled well beyond the position marked for the intended sample volume. The syringe was then detached from the cartridge and swung in an arc to force the liquid away from the tip while forcing the entrapped air toward the tip. The air was subsequently expelled, along with excess liquid, into a waste bag by the forward displacement of the plunger. Finally, the debubbled syringe was capped and stored for ground analysis.

Results

Results from the gravimetric analyses of the samples collected in-flight are given in Tables 4 and 5. The average volume of liquid contained in the 3-mL and 10-mL syringes that were capped as-filled (i.e., not debubbled) are given in Table 4. The volume of liquid was calculated from mass using the density of water (1 g/mL), and the volume of air introduced into each syringe by the reagent cartridge was obtained by subtracting the liquid sample volume from the total volume (either 3.0 or 10.0 mL). The results from samples that were manipulated to collect bubble-free 1.0 and 10.0-mL samples are presented in Table 5.

As previously mentioned, the concentration of sodium in each sample collected during the flight was determined by ICP-MS analysis. The average concentration for each sample type is reported in Table 6.

Discussion

According to the data reported in Table 4, the addition of a reagent cartridge in-line between the sample bag and the syringe introduces up to 1.9 mL of air during

sample collection. In a few cases, the Luer slip fitting between the cartridge and the sample bag was not secure, causing those syringes to be filled with ambient air rather than liquid from the sample bag. This problem occurred with four of the samples, which were therefore excluded from the data reported in Tables 4-6. To avoid this problem in the future, cartridges with Luer Lok fittings on both ends are recommended.

Despite this minor issue, the data in Table 5 clearly show that, while filling through a cartridge introduces air into the syringe, it is possible to collect a bubble-free sample by removing the air from the syringe. Manually centrifuging the syringe by swinging it in an arc was a very effective method for removing air bubbles from a liquid sample in both the 10-mL and 3-mL syringes. Figure 4 shows the bubble distribution in a 3-mL syringe filled through a reagent cartridge containing glass wool.

The results of the ICP-MS analyses indicate that the glass wool introduces much more NaCl into the sample than does the filter paper. This is to be expected given that each glass wool disk contained approximately 70 times as much NaCl as a filter paper disk. However, the 3-mL syringes filled through the glass wool disks had NaCl concentrations 80-90 times higher than those filled through the filter paper disks. The difference in the 10-mL syringes is even greater, with the glass wool producing NaCl solutions 100-140 times as concentrated as those produced by filter paper disks. Taken together, these data suggest that glass wool is a more efficient means of reagent introduction than filter paper.

The variability in NaCl delivery, however, is also higher for glass wool than for filter paper. Two likely reasons for this increase in standard deviation are: 1) the glass wool disks, which are prepared by the user, have far more variability in thickness, density, etc. than the filter paper, which can be used as-received, and 2) the solution used to prepare the glass wool disks was a slurry and therefore not as uniform as the homogenous solution used to impregnate the filter paper. It is important to note also that syringes were filled at varying speeds in order to observe the effect, if any, on bubble introduction, and this could very well have contributed to the variation in reagent introduction with both types of media. It was determined that in future experiments, syringes should be filled slowly, as this both increases reagent delivery and reduces bubble dispersion.

4. Conclusions

Several important conclusions can be drawn from this series of flight experiments. In Flight 1, we demonstrated that manual manipulation of water sample bags is effective for air/water separation. Specifically, 1.0-mL and 10.0-mL samples of effectively bubble-free water can be collected in syringes in microgravity starting with water samples containing up to 50% air, the highest amount tested. During Flights 2 and 3, we showed that silver(I) and iodine analyses performed in-flight on samples collected from bags containing up to 47% air agreed with ground results obtained using bubble-free samples. These results indicate that both methods should be viable approaches for on-orbit water quality monitoring during

spaceflight. The next phase of this work will focus on the development and deployment of an experimental water quality test kit for use on ISS or Shuttle.

During Flight 4, both 3-mL and 10-mL syringes were filled with bubble-free 1.0-mL and 10.0-mL liquid samples despite the introduction of up to 1.9 mL of air from a cartridge used to introduce reagents. This is an important first step in the development of microgravity-compatible test procedures for total iodine, total silver, nickel, and formaldehyde.

References

(1) Fritz, J. S. *Analytical Solid-Phase Extraction*; Wiley-VCH: New York, 1999.

(2) Arena, M. P.; Porter, M. D.; Fritz, J. S. *Anal. Chem.* **2002**, *74*, 185-190.

(3) Arena, M.; Porter, M.; Fritz, J.; Mudgett, P.; Rutz, J.; Schultz, J. *32th International Conference on Environmental Systems* **2002**, *SAE Technical Paper #2002-01-2535.*

(4) Arena, M. P.; Porter, M. D.; Fritz, J. S. *Anal. Chim. Acta* **2003**, *482*, 197-207.

(5) Dias, N. C.; Gazda, D. B.; Fritz, J. S.; Porter, M. D.; Rutz, J.; Mudgett, P.; Schultz, J. *34th International Conference on Environmental Systems* **2004**, *SAE Technical Paper #2004-01-2539.*

(6) Fritz, J. S.; Arena, M. P.; Steiner, S. A.; Porter, M. D. *J. Chromatogr. A* **2003**, *997*, 41-50.

(7) Gazda, D. B.; Lipert, R. J.; Fritz, J. S.; Porter, M. D.; Rutz, J.; Mudgett, P.; Schultz, J. *33th International Conference on Environmental Systems* **2003**, *SAE Technical Paper #2003-01-2406*.

(8) Gazda, D. B.; Fritz, J. S.; Porter, M. D. *Anal. Chim. Acta* **2004**, *508*, 53-59.

(9) Gazda, D. B.; Lipert, R. J.; Fritz, J. S.; Porter, M. D. *Anal. Chim. Acta* **2004**, *510*, 241-271.

(10) Gazda, D. B.; Fritz, J. S.; Porter, M. D. *Anal. Chem.* **2004**, *76*, 4881-4887.

(11) Hazen-Bosveld, A. A.; Fritz, J. S.; Porter, M. D. *35th International Conference on Environmental Systems* **2005**, *SAE Technical Paper #2005-01-3063*.

(12) Wendlandt, W. W.; Hecht, H. G. *Reflectance Spectroscopy*; Inter-science: New York, 1966.

(13) Kortum, G. *Reflectance Spectroscopy: Principles, Methods, Applications*; Springer-Verlag: New York, 1969.

(14) Blitz, J. P. In *Modern Techniques in Applied Molecular Spectroscopy*; Mirabella, F. M., Ed.; John Wiley & Sons, Inc.: New York, 1998, pp 185-219.

(15) *Standard methods for the examination of water and wastewater*, 18th ed.; American Public Health Association: Washington DC, 1992.

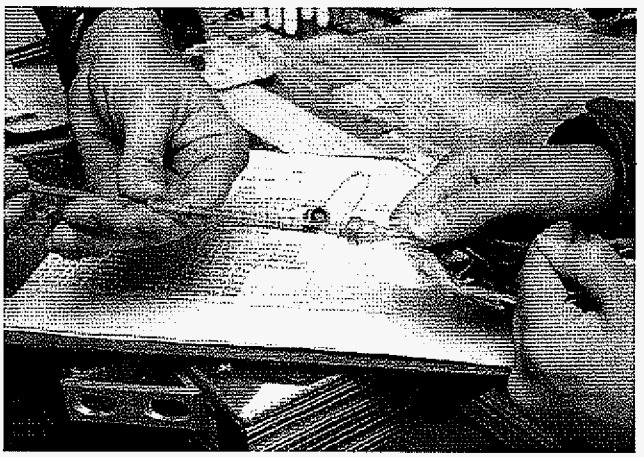

Figure 1. Filling a 1-mL syringe in-flight from a manually debubbled sample bag.

Table 1. Comparison of mass of liquid contained in syringes filled in flight from bags containing air/water mixtures to syringes filled on ground from bubble-free samples.

	1-mL Syringes		10-mL Syringes		25-mL Syringes	
	Flight	Ground	Flight	Ground	Flight	Ground
Average mass (g)	0.9932	1.0003	9.8983	9.9893	9.7680	9.9448
Std. Dev.	0.0177	0.0045	0.0686	0.0269	0.2503	0.0864
RSD	1.8%	0.45%	0.69%	0.27%	2.56%	0.87%
Error	-0.68%	+0.03%	-1.02%	-0.11%	-2.32%	-0.55%

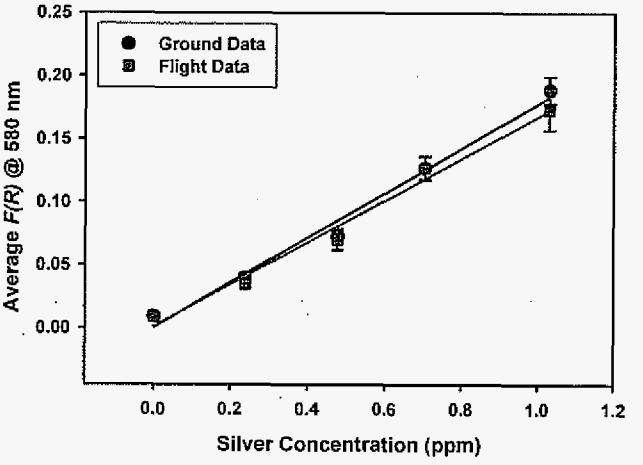

Figure 2. Comparison of the data from ground and flight testing of silver(I) by C-SPE.

Table 2. Comparison of the calibration equations from ground and flight testing of silver(I) by C-SPE.

	Calibration Equation	R^2	LOD (ppb)
Flight	$[Ag^+] = 6.00F(R) - 0.0066$	0.984	28.5
Ground	$[Ag^+] = 5.62F(R) - 0.019$	0.986	21.8

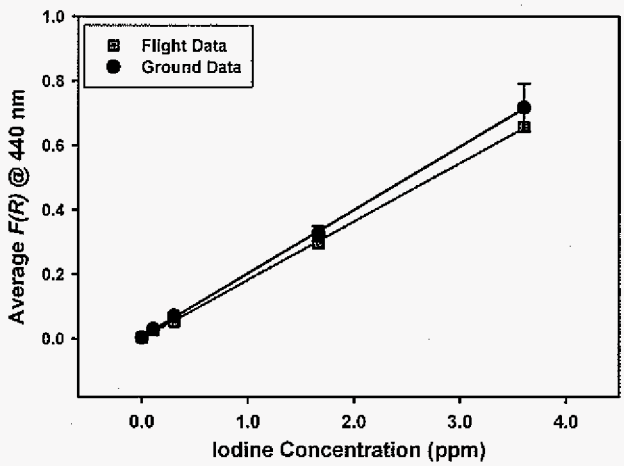

Figure 3. Comparison of the data from ground and flight testing of iodine (I_2) by C-SPE.

Table 3. Comparison of the calibration equations from ground and flight testing of iodine (I_2) by C-SPE.

	Calibration Equation	R^2	LOD (ppb)
Flight	$[I_2] = 5.52F(R) - 0.010$	0.9996	7.3
Ground	$[I_2] = 5.09F(R) - 0.033$	0.9997	4.9

Table 4. Average volumes of liquid and air introduced into 3-mL and 10-mL syringes when filled to the mark through reagent cartridges.

	3-mL Syringes				10-mL Syringes			
	Glass Wool		Filter Paper		Glass Wool		Filter Paper	
	liq.	air	liq.	air	liq.	air	liq.	air
Vol. (mL)	1.20	1.80	1.85	1.15	8.093	1.907	8.52	1.48
Std. Dev.	0.46	0.46	0.32	0.32	0.083	0.083	0.16	0.16

Table 5. Average volumes of 1.0 and 10.0-mL samples collected by filling 3-mL and 10-mL syringes through reagent cartridges and manually debubbling.

	3-mL Syringes		10-mL Syringes	
	Glass Wool	Filter Paper	Glass Wool	Filter Paper
Vol. (mL)	1.016	0.999	9.807	9.60
Std. Dev.	0.016	0.034	0.078	0.40

Table 6. Results from ICP-MS analysis of sodium concentration in all samples collected through reagent cartridges in flight.

	3-mL Syringes				10-mL Syringes			
	Glass Wool		Filter Paper		Glass Wool		Filter Paper	
	AF*	DB*	AF	DB	AF	DB	AF	DB
[Na^+] (ppm)	5184	4302	57	54	1165	1122	8.2	11.02
Std. Dev.	2238	1844	22	10	141	273	1.2	0.64

*AF: as filled; DB: debubbled

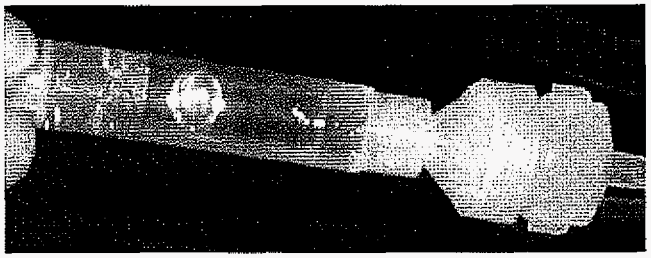

Figure 4. A 3.0-mL syringe after filling through glass wool cartridge in microgravity.

CHAPTER 2. DETERMINATION OF COLLOIDAL AND DISSOLVED SILVER IN WATER SAMPLES USING COLORIMETRIC-SOLID PHASE EXTRACTION

A paper to be submitted to *Analytica Chimica Acta*

April A. Hill, Robert J. Lipert, and Marc D. Porter*†

Iowa State University, Institute for Combinatorial Discovery, Departments of Chemistry and of Chemical and Biological Engineering, and Ames Laboratory-U.S. DOE, Ames, IA 50011-3020

†Department of Chemistry and Chemical Engineering, University of Utah, Salt Lake City, UT 84108

*Corresponding author

Abstract

A rapid, simple method for the determination of ionic and colloidal silver in water has been developed. The increased antibiotic resistance exhibited by many bacteria today has led to a resurgence in the use of silver as an antibacterial agent in applications ranging from washing machine additives to the drinking water treatment system on the International Space Station (ISS). However, amid growing concerns that the introduction of colloidal silver into water systems may kill beneficial bacteria and aquatic organisms and may pose risks to human health, the US EPA and FDA have recently issued regulations regarding its use. As part of an ongoing project with NASA, we have developed a rapid, simple method for determining silver, both dissolved and colloidal, in aqueous samples between 0.1-1 ppm, which spans the ISS potable water target level of 0.3-0.5 ppm total silver. The method is based on colorimetric solid-phase extraction (C-SPE) and involves the extraction of silver(I)

from water samples by passage through a solid-phase membrane that has been impregnated with the colorimetric reagent DMABR (5-[4-(dimethylamino)benzylidene]rhodanine). Silver(I) exhaustively reacts with DMABR to form a colored compound, which is quantified using a handheld diffuse reflectance spectrophotometer. Total silver is determined by first passing the sample through an inline cartridge containing Oxone, which oxidizes colloidal silver to dissolved silver(I). The method, which requires less than 2 min to fully complete and uses only ~1 mL of sample, has been validated by comparison with ICP-MS analysis of a water sample from ISS, which contains both dissolved and colloidal silver. Potential earth-bound applications are also discussed.

1. Introduction

Silver has been used for its antimicrobial properties since the ancient Romans employed silver coins to treat water supplies.[1] The increased antibiotic resistance exhibited by many bacteria today has led to a resurgence in the use of silver as a biocidal agent. In fact, antimicrobial coatings of colloidal silver are already being used in a wide variety of applications, including deodorizing shoe inserts, washing machines, and wound dressings.[1,2] Though no pathogen has yet been found to be resistant to silver, there are risks associated with its use. High levels of silver can kill human cells, which, in the case of wound care, could slow the healing process. There are also risks associated with ingestion of silver. Argyria, for example, is a condition characterized by a permanent blue-gray discoloration of the skin.[3]

In light of these issues, the US EPA recently classified colloidal silver, such as that used in washing machines, as a pesticide. Moreover, the FDA ruled that over-the-counter products containing silver colloids or salts are not generally recognized as safe for human use.[2,4] These rulings highlight the need for rapid, simple, field-deployable methods for monitoring colloidal silver concentrations in liquid samples. Test kits for the determination of silver in water samples are commercially available, most of which are based on the use of colorimetric chemistry, with readout accomplished by visual color matching of either test strips or liquid samples. However, these methods typically require large sample volumes (e.g., 10-100 mL) and deliver only semi-quantitative results. Furthermore, to our knowledge, very few of these methods can detect colloidal silver, and they rely on strong acids, which are corrosive and hazardous, to do so.[5-7]

This paper details the development of a method capable of determining both colloidal and ionic silver in water samples in less than 2 min. Though this method would be useful for monitoring colloidal silver concentrations in many of the aforementioned earth-bound applications, it was actually developed as a means to monitor silver concentrations in the potable water supply on-board the International Space Station (ISS), which employs electrolytically generated silver as a biocidal agent. While ISS documentation lists a target level of 0.3-0.5 ppm silver,[8] there is no method for monitoring the silver concentration during flight. In fact, the current method of monitoring spacecraft water quality relies on samples that are collected on ISS and returned to Earth for analysis. The gap between sample collection and

analysis can, however, span several months, which prevents the timely implementation of correction scenarios. Consequently, the development of rapid, on-board methods for monitoring trace levels of critical components in spacecraft drinking water supplies is a priority for NASA. These methods must have sufficient selectivity and sensitivity to detect analytes at low concentrations, and also be user-friendly, small, lightweight, and capable of operation in microgravity. Recent reports from our laboratory have demonstrated that colorimetric solid-phase extraction (C-SPE) meets many of these requirements.[9-24]

C-SPE typically involves the extraction of an analyte from a water sample onto a solid-phase membrane that has been impregnated with a colorimetric reagent. While flowing through the membrane, the analyte reacts with the colorimetric reagent, causing the membrane to change color. Using diffuse reflectance spectroscopy (DRS) as a readout technique, quantification of the analyte is accomplished via a calibration plot of the Kubelka–Munk function against analyte concentration.[25,26] The complete procedure usually requires less than 2 min per analysis. Importantly, impregnating the extraction membranes with the colorimetric reagents eliminates the need to handle solvents and chemicals throughout sample workup, enabling C-SPE to function in a "reagentless" format, thereby minimizing exposure to hazardous materials. In addition, the use of a solid-phase extraction membrane results in concentration factors on the order of 1000, enabling C-SPE to detect analytes at very low concentrations.[27]

To date, our laboratory has developed C-SPE methods for the NASA-based biocides iodine (I_2) and silver(I), and the heavy metals nickel(II), chromium(VI), copper(II), and iron(III).[9,10,14,20] We recently reported the development of a C-SPE method for determining formaldehyde, which is the first application of C-SPE to the detection of an organic contaminant.[24] We have also carried out assessments of the performance of these methods in microgravity,[13,18,21] which have shown excellent agreement between flight and ground-based analyses of iodine and silver(I).[22,23]

The existing C-SPE method for silver(I) uses the colorimetric reagent DMABR (5-[4-(dimethylamino)benzylidene]rhodanine).[10] However, DMABR does not react with colloidal silver. This limitation is important because the silver that is added as a biocide to the water supply on the International Space Station (ISS) is present in both dissolved and colloidal forms.[28] Thus, to detect colloidal silver using our DMABR-based method, an oxidizing agent must be added to the water sample to exhaustively convert colloidal silver to silver(I). This paper presents the development of a C-SPE method for determining both colloidal and dissolved silver (as silver(I)) using the oxidizing agent Oxone.

Oxone, a well-known oxidizing agent, was investigated for use in this analysis for a number of reasons: (1) it is readily soluble in water, (2) it is considered non-toxic, as evidenced by its popularity as an ingredient in denture cleansers and swimming pool disinfectants,[29] and (3) it is already approved for use on-board NASA spacecraft, where it is employed in the pretreatment of urine for storage in the waste collection system.[30] The active ingredient of Oxone is potassium monopersulfate

($KHSO_5$), a neutralization salt of peroxymonosulfuric acid. Since Oxone is slightly acidic, it is often buffered to near-neutral pH by the addition of alkaline salts, such as sodium carbonate, when used in cleanser formulations.[29] Our technique was devised to include such a buffering system as a means to reduce the adverse effects of Oxone on the silver(I)-sensitive membranes. Specifically, sodium carbonate was introduced into the C-SPE analysis after the oxidation step to neutralize the pH before passing the sample through the membrane. The resulting C-SPE method determines the total concentration of colloidal and dissolved silver in the range of 0.1 to 1 ppm in less than 2 min, and, when combined with the existing method for determining silver(I), provides the capability to determine colloidal silver in the presence of dissolved silver.

2. Experimental

2.1. Reagents and chemicals

All solutions were prepared daily with deionized water that was purified by a Millipore Milli-Q water purification system.

2.1.1. Silver(I) sample solutions

Solutions with dissolved silver concentrations between 0.25 and 1.0 ppm were prepared in Nalgene bottles by diluting the appropriate mass of a 996 ppm silver atomic absorption standard (Sigma-Aldrich) with deionized water.

2.1.2. Colloidal silver sample solutions

Silver nanoparticles, 20, 40, 60, and 80-nm in diameter, were purchased from Ted Pella at respective concentrations of 7.0×10^{11}, 9.0×10^{10}, 2.6×10^{10}, 1.1×10^{10} particles/mL. These sizes were chosen to mimic the range of silver colloid sizes present in water with electrolytically generated silver.[28] The actual concentration of silver (as Ag(I)) in each of the colloidal suspensions (hereafter referred to as solutions) was determined using ICP-MS. An aliquot of each solution was adjusted to pH 2 using nitric acid and then diluted by a factor of 10 with deionized water. The concentrations were determined using a calibration plot generated from dilutions of the aforementioned atomic absorption standard for silver. The total concentration (within 2.55% or less) of silver in each solution was determined to be 6.05, 5.91, 5.96, and 5.77 ppm for the 20, 40, 60, and 80-nm particles, respectively. Colloidal silver samples were prepared by diluting either the 80-nm colloidal solution or a mixture containing equal volumes of each of the four colloidal solutions with deionized water. The amount of silver present in each sample solution was also verified by ICP-MS.

2.1.3. Extraction cartridges

A solution of DMABR (Aldrich), the colorimetric reagent for silver(I), was prepared by dissolving 0.060 g DMABR in 20 mL of dimethyl formamide in a 100-mL volumetric flask. After sonicating for ~5 min to dissolve the DMABR, the solution was brought to volume using methanol. A second solution was prepared by pipetting

3.0 g of Brij 30 surfactant (Aldrich) into a Nalgene bottle and bringing the total mass to 100 g with deionized water.

These solutions were used to impregnate 3M Empore SDB-XC (polystyrene-divinylbenzene) 47-mm extraction membranes. Each membrane was placed into an all-glass filter holder assembly (Millipore), and 10.0 mL of the DMABR solution was pipetted into the funnel. Using a vacuum pump, a pressure differential of ~1 inch of Hg was applied to drive the solution through the membrane. After the DMABR solution had passed through the membrane, the pressure differential was maintained for another 10 s to remove residual liquid. The vacuum pump was then turned off and the funnel removed. A second funnel was clamped in place and 5.0 mL of the Brij 30 solution was added via a pipette. The use of two funnels prevents mixing of the aqueous and organic solutions, which leads to the formation of DMABR particulates that deposit on the membrane surface as red spots. A vacuum-derived pressure of ~3.5 in Hg was applied to pull the Brij 30 solution through the membrane. This pressure differential was subsequently increased to ~20 in Hg (the maximum attainable pressure differential) for 30 s to dry the membrane.

After reagent impregnation, the silver(I)-sensitive membranes were fully dried by storage in a dark drawer overnight (~16 h). The dried membranes were then cut into 13-mm disks using a cork borer. Next, each disk was placed on top of the support screen in the bottom portion of a Swinnex polypropylene filter holder (Millipore). The holder was assembled by sealing against a silicone gasket (11-mm

inner diameter) that both defines the area of the disk exposed to the water sample and forms an internal seal within the cartridge.

2.1.4. Oxone cartridges

Two types of Oxone-impregnated disks were prepared by pipetting a 1.0-mL aliquot of either (A) 60 mg/mL or (B) 300 mg/mL Oxone (Aldrich) in deionized water onto a 47-mm diameter glass fiber filter (Millipore), in a 50-mm glass Petri dish. These filters were dried in an oven at 110 °C for ~1 h before being cut into 13-mm disks and loaded into Swinnex filter holders as described in Section 2.1.3. These holders, referred to as Type A or Type B Oxone cartridges, contained ~6 and ~25 mg Oxone, respectively.

2.1.5. Sodium carbonate cartridges

A 2.0-mL aliquot of 200 mg/mL sodium carbonate in deionized water was pipetted onto a 45-mm diameter media pad (Millipore) in a 50-mm glass Petri dish. The pad was placed in an oven at 110 °C until the excess liquid had evaporated, leaving a saturated pad (~ 20 min). The pad was then cut into 9-mm disks using a cork borer. These disks, which contained ~16 mg sodium carbonate, were returned to the Petri dish and dried in the oven at 110 °C for ~2 h. The disks were loaded into Swinnex filter holders as described in Section 2.1.3 with one exception; i.e., in order to accommodate the thickness of the pad, the support screen was removed from the bottom half of each holder and the disk mounted in its place.

2.2. Instrumentation

A BYK-Gardner color-guide sphere (d/8°) diffuse reflectance spectrophotometer (Model LCB-6830) was used to measure the diffuse reflectance (DRS) spectra of the disks after passage of the aqueous silver(I) samples. This hand-held spectrophotometer, which is small, lightweight, and battery-powered, can collect reflectance data in under 2 s over the visible spectral range (400-700 nm) in 20-nm intervals.[13] After a sampling session, the DRS data files are downloaded to a personal computer and analyzed using BYK-Gardner QC-Link software that was modified in-house to calculate the Kubelka-Munk function (*F(R)*), which is given by Equation 1,[25]

$$F(R) = (1 - R)^2 / 2R \quad (1)$$

where R is the diffuse reflectance measured relative to a reflectance standard. We note that the *F(R)* at a given wavelength is directly related to the concentration of the complex in the membrane, C, by Equation 2,

$$F(R) = 2.303\varepsilon C / s \quad (2)$$

where ε is the molar absorptivity of the colorimetric product and s is the scattering coefficient of the sample surface, both of which are assumed to be constant throughout an analysis.[26]

3. Method Development

3.1. Existing C-SPE method for silver(I)

A schematic of the C-SPE method for silver(I) is illustrated in Figure 1a. Specifically, a 1.0-mL aqueous sample is collected in a 1-mL polypropylene syringe and passed through an extraction cartridge containing a DMABR reagent disk, after which a second syringe is used to pass ~60 mL of air through the cartridge to dry the disk. The cartridge is then opened and the DRS spectrum of the reagent disk is acquired in under 2 s using the spectrophotometer. Representative DR spectra from a C-SPE analysis of silver(I) are also presented in Figure 1b.

3.2. Initial assessments of Oxone as an oxidizing agent

To determine the efficiency of Oxone as an oxidizing agent for colloidal silver, various amounts of Oxone were added to individual aliquots of a solution containing ~0.5 ppm colloidal silver (80 nm). After stirring to dissolve the Oxone, each colloidal silver sample was allowed to react for 1 h (a more thorough determination of reaction time is discussed below), after which the concentration of silver(I) was determined by the existing C-SPE method (Figure 1a). Using a calibration plot constructed from *F(R)* at λ= 580 nm vs. concentration of silver(I) from a series of standard solutions, the amount of silver(I) formed in the oxidized colloidal samples was determined. A comparison of the amount of silver(I) detected by C-SPE to the total amount of silver determined by ICP-MS indicates that the optimum amount of oxidizing reagent needed to completely form silver(I) from colloidal silver is 6 mg/mL. Above this concentration, however, excess Oxone causes the DMABR disks to

visually fade rapidly from orange-yellow to white. This observation suggests that excess Oxone can oxidize the DMABR on the membrane.

To maintain the "reagentless" aspect of C-SPE methods, the Oxone was then immobilized and loaded into filter holders as described in Section 2.1.4 (Type A). A total silver analysis could then be carried out by collecting a sample into a syringe via the Type A Oxone cartridge, which delivers ~6 mg/mL Oxone to the sample. To determine the time required for the Oxone to dissolve the colloidal silver in this experiment, a test solution was prepared by diluting 80-nm silver colloids (the largest particles tested, and therefore expected to be slowest to dissolve) in deionized water to give a concentration of 0.57 ppm silver. Samples of this solution were collected by filling 3-mL polypropylene syringes with ~1.1 mL of the test solution via the Type A Oxone cartridge, which has a dead volume of ~1 mL. Each syringe was capped and shaken vigorously for 20 s to thoroughly mix the contents. The samples were then allowed to react in the syringes for various amounts of time before the air and excess liquid were expelled, leaving a 1.0-mL sample. This sample was then passed through an extraction cartridge, followed by ~60 mL of air, and the DRS spectrum of the disk acquired. The results, plotted in Figure 2, indicate that the method requires ~1 h to fully dissolve 80-nm silver colloids. Because C-SPE analyses typically require only 1 to 2 min, we sought next to increase the rate of the oxidation step, and thereby reduce assay time.

3.3. Increasing oxidation rate using excess Oxone

An obvious method for speeding up the oxidation step was to increase the concentration of Oxone in the samples. However, as previously mentioned, excess Oxone oxidizes the DMABR on the extraction disks, causing a rapid loss of color. Therefore, if excess Oxone is introduced into the samples to speed the oxidation of colloidal silver, it must be neutralized before the solution can be passed through the extraction disk. As previously mentioned, Oxone, which is slightly acidic, is often blended with alkaline salts in order to maintain neutral pH. A specific example of this is the use of sodium carbonate and Oxone in a 1:4 ratio by mass to create a pool disinfectant with neutral pH.[29] Initial tests of the usefulness of this combination of sodium carbonate and Oxone in the analysis of total silver by C-SPE showed that (1) much higher concentrations of Oxone can be used without any visible deterioration of the extraction disk, and (2) the rate of conversion of colloidal silver to dissolved silver increases with the concentration of Oxone.

It is important to note that adding the sodium carbonate before the colloidal silver had been oxidized greatly reduced the amount of silver(I) produced at short reaction times. This situation can be explained by the fact that Oxone relies on peracid chemistry to oxidize the colloidal silver, and the oxidation is thereby enhanced by acidic conditions, as illustrated by the reaction shown in Equation 3.[29]

$$HSO_5^- + 2H^+ + 2e^- \longrightarrow HSO_4^- + H_2O \qquad E^o = +1.44\ V\ (NHE) \qquad (3)$$

According to Equation 3, the oxidation strength of Oxone depends on the hydrogen ion concentration. In the case of pool disinfection, which is a continuous

process (i.e. oxidation does not need to be fast), the use of near-neutral pH keeps the pool environment safe for people while still allowing for the oxidative prevention of microbial growth. However, for the current application, rapid oxidation is required, so the sodium carbonate is not added until the oxidation is complete. As such, sodium carbonate affects the sample in two ways; it neutralizes the pH of the sample and decreases the oxidation strength of the remaining Oxone, both of which affect the color development of the silver(I)-sensitive membrane.

Based on the results of these initial tests, Oxone and sodium carbonate were immobilized onto inert media and loaded into cartridges as described in Sections 2.1.4 (Type B) and 2.1.5. Notably, Oxone and sodium carbonate are not present in the reagent cartridges in the 4:1 ratio recommended for pool disinfection. Because sodium carbonate is not as readily soluble in water as Oxone, the concentration present in the reagent cartridge was increased until the final pH of samples analyzed by the procedure described in Section 3.4 were equivalent to that of typical potable water samples (i.e., near pH 6).

3.4. C-SPE method for total silver using Oxone and sodium carbonate

The procedure for the C-SPE determination of total silver using the Oxone/sodium carbonate method is illustrated in Figure 1a. An Oxone cartridge (Type B) is connected to a 3-mL Luer Lock polypropylene syringe and aqueous samples containing colloidal silver are drawn into the syringe, passing through the cartridge, and dissolving the ~25 mg of Oxone. Approximately 1.1 mL of sample is collected in each syringe, in addition to the air (~1 mL) that occupies the dead

volume of the Oxone cartridge. The Oxone cartridge is then removed and the syringe capped and shaken by hand for 20 s to disperse the Oxone and allow it to react with the colloidal silver. The air and excess liquid are then expelled from the syringe to meter a 1.0-mL volume. The metered sample is first passed through a sodium carbonate cartridge and then through an extraction cartridge, which are connected in series. Next, the sample syringe is disconnected from the cartridge assembly and replaced by a 60-mL syringe. Approximately 60 mL of air is passed through the two-cartridge assembly to force any sample occupying the cartridge dead volume through the extraction disk, at the same time drying the disk. Finally, the holder is disassembled and the DRS spectrum of the reagent disk containing extracted silver(I) is acquired.

4. Results and Discussion

4.1. Calibration of C-SPE method for total silver

The procedure for determining total silver by C-SPE, described in Section 3.4, is both rapid and simple, requiring less than 2 min to complete. The calibration plot shown in Figure 3 was obtained by performing this procedure in triplicate on solutions containing silver(I) at concentrations up to 1.0 ppm. For comparison, a typical response obtained from the C-SPE method for silver(I) over this concentration range is also presented. Since both calibration plots in Figure 3 were generated using silver(I) solutions, the deviation between the two plots is an indication of the effects of Oxone and sodium carbonate on the membranes. In spite of the slight deviation, the new method gives a linear response over the

concentration range of interest for NASA water quality monitoring, with a calculated limit of detection (using three times the standard deviation of the blank) of 0.1 ppm silver. This value is comparable to the LOD of the silver(I) method, which is 0.06 ppm silver(I).

4.2. Validation of C-SPE method for total silver

To evaluate the developed method for use with samples containing colloidal silver, three samples were created by first mixing 2.0-mL aliquots of each silver colloid solution (20, 40, 60, and 80-nm), and then diluting the mixture (~6 ppm silver) with deionized water to give three sample solutions with approximate concentrations of 1, 0.5, and 0.15 ppm silver. These samples were analyzed by ICP-MS and by the total silver C-SPE method. For the ICP-MS analysis, the average of ten replicate measurements was used to calculate the concentration using a calibration plot. Using the equation of the total silver calibration plot in Figure 3, the concentration of silver detected by C-SPE in each of the colloidal samples was calculated from the average *F(R)* value at λ = 580 nm (n = 3). As evident in Table 1, the values given by the C-SPE method are all within 9% of those given by ICP-MS, demonstrating the effectiveness of the technique.

Interestingly, the data in Table 1 show that the error in the C-SPE measurement (i.e., as compared to the ICP-MS result) increases with the concentration of colloidal silver in the sample. We attribute this finding to the fact that samples with higher concentrations of colloidal silver reduce more of the Oxone present in the sample, leading to a relative excess of sodium carbonate. The result

is a slight increase in the alkalinity of the sample, which in turn causes a slight change in the color of the membrane. This is a minor issue, however, since the accuracy of the method is within 10%, a level of agreement comparable to that achieved for other C-SPE methods.

As a further validation of the C-SPE method for total silver, a sample of potable water from ISS, which was returned to Earth by the shuttle Endeavour (Mission STS-97) on December 11, 2000, and stored at ~5 °C, was analyzed by ICP-MS (n = 10) and by both the silver(I) and total silver C-SPE methods (n = 3). The results of this analysis, presented in Table 2, demonstrate that the new method can rapidly detect all of the silver present in the potable water supplies of ISS. Moreover, the concentration given by the silver(I) C-SPE method can be subtracted from that given by the total silver method to determine the concentration of colloidal silver in the presence of silver(I). Though not shown in Table 2, the difference between the concentration given by the total silver C-SPE method and that given by the ICP-MS method is ~0.4 %. This is consistent with the ~0.6 % reported in Table 1 for Sample 3, which has a similar concentration of colloidal silver (~0.12 ppm), indicating the validity of the method.

5. Conclusions

A rapid, simple method for determining total silver has been developed. This method uses Oxone, a relatively safe and readily available oxidizing agent, to convert colloidal silver to silver(I), which is then detected using C-SPE. The entire

procedure requires less than 2 min, is extremely simple, and poses minimal hazards to the user, making this method an attractive option for a wide variety of applications. The method is accurate, providing close (within 9%) agreement with ICP-MS values over the concentration range of interest. Moreover, by combining this new method with the C-SPE analysis of silver(I) previously developed in our laboratory, colloidal silver concentrations can be determined in the presence of silver(I), thus enabling a rapid determination of silver speciation in aqueous samples. Regarding the original motivation for this project, the utility of the total silver C-SPE method for monitoring the biocidal silver present in spacecraft water supplies has been validated. We are currently planning experiments to test the performance of this method in microgravity aboard NASA's C-9 aircraft. However, there is also considerable potential for earth-bound applications of this method, based on the widespread popularity of colloidal silver as a biocidal agent in recent years, coupled with the fact that this method is a viable alternative to the more expensive (ICP-MS) and less effective (test strip) methods currently available.

Acknowledgements

The authors would like to thank Jeff Rutz, Dan Gazda and John Schultz of Wyle Laboratories, Houston, TX, USA for their insightful discussions. This work was supported by NASA contract NAG91510. The Ames Laboratory is operated by Iowa State University under U.S. Department of Energy contract DE-AC02-07CH11358.

References

(1) Halford, B. In *Chemical & Engineering News, 84(16)*, 2006, pp 35-36.

(2) Morrissey, S. In *Chemical & Engineering News, 84(49)*, 2006; Vol. 84, pp 14.

(3) Brandt, D.; Park, B.; Hoang, M.; Jacobe, H. T. *J Am Acad Dermatol* 2005, *53*, S105-S107.

(4) *Department of Health and Human Services, Food and Drug Administration, Federal Register* 1999, *64*, 44653-44658.

(5) LaMotte Silver Test Kit Information, http://www.lamotte.com/pages/common/pdf/instruct/3617.pdf, 2007.

(6) Hach RapidSilver Visual Silver Test Kit Manual, http://www.hach.com/fmmimghach?/CODE%3A2674588912%7C1, 2007.

(7) HMT Silver Test Kit: How to Test, http://www.heavymetalstest.com/_agtest.php, 2007.

(8) *Technical Requirements Specification Document for the ISS Water Transfer Hardware, JSC-39223, NASA-JSC, June 1999.*

(9) Arena, M. P.; Porter, M. D.; Fritz, J. S. *Anal. Chem.* 2002, *74*, 185-190.

(10) Arena, M. P.; Porter, M. D.; Fritz, J. S. *Anal. Chim. Acta* 2003, *482*, 197-207.

(11) Dias, N. C.; Fritz, J. S.; Porter, M. D. *35th International Conference on Environmental Systems, Rome, Italy* 2005, *SAE Technical Paper #2005-01-3065.*

(12) Dias, N. C.; Gazda, D. B.; Fritz, J. S.; Porter, M. D. *34th International Conference on Environmental Systems, Colorado Springs, CO* 2004, *SAE Technical Paper #2004-01-2539.*

(13) Gazda, D. B.; Lipert, R. J.; Fritz, J. S.; Porter, M. D.; Rutz, J.; Mudgett, P.; Schultz, J. *33rd International Conference on Environmental Systems, Vancouver, B.C., Canada* 2003, *SAE Technical Paper #2003-01-2406.*

(14) Gazda, D. B.; Fritz, J. S.; Porter, M. D. *Anal. Chim. Acta* 2004, *508*, 53-59.

(15) Gazda, D. B.; Fritz, J. S.; Porter, M. D. *Anal. Chem.* 2004, *76*, 4881-4887.

(16) Nordling, J.; Lipert, R. J.; Porter, M. D.; Gazda, D. B. *35th International Conference on Environmental Systems, Rome, Italy* 2005, *SAE Technical Paper #2005-01-2891.*

(17) Shih, C. J.; Dias, N. C.; Porter, M. D. *35th International Conference on Environmental Systems, Rome, Italy* 2005, *SAE Technical Paper #2005-01-2890.*

(18) Arena, M. P.; Porter, M. D.; Fritz, J. S.; Mudgett, P.; Rutz, J.; Schultz, J. *32nd International Conference on Environmental Systems, San Antonio, TX* 2002, *SAE Technical Paper #2002-01-2535.*

(19) Dias, N. C.; Porter, M. D.; Fritz, J. S. *Anal. Chim. Acta* 2006, *558*, 230-236.

(20) Fritz, J. S.; Arena, M. P.; Steiner, S. A.; Porter, M. D. *J Chromatogr. A* 2003, *997*, 41-50.

(21) Ponton, L. M.; Gazda, D. B.; Lipert, R. J.; Fritz, J. S.; Porter, M. D.; Rutz, J.; Mudgett, P.; Dungan, D.; Schultz, J. *33rd International Conference on Environmental Systems, Vancouver, B.C., Canada* 2003, *SAE Technical Paper #2003-01-2408.*

(22) Porter, M.; Arena, M.; Weisshaar, D.; Mudgett, P.; Rutz, J.; Benoit, M.; Colorimetric Solid Phase Extraction Measurements of Spacecraft Drinking Water Contaminants in: *KC-135 Postflight Report*, 2004.

(23) Porter, M. D.; McCoy, J. T.; Hazen-Bosveld, A. A.; Lipert, R. J.; Nordling, J.; Shih, C. J.; Gazda, D. B.; Rutz, J.; Straub, J.; Schultz, J.; Alverson, J.; Colorimetric Solid Phase Extraction Measurements of Spacecraft Drinking Water Contaminants in: *C-9 Postflight Report*, 2006.

(24) Hill, A.; Lipert, R. J.; Fritz, J. S.; Porter, M. D. *manuscript in preparation* 2007.

(25) Kortum, G. *Reflectance Spectroscopy: Principles, Methods, Applications*; Springer: New York, 1969.

(26) Blitz, J. P. In *Modern Techniques in Applied Molecular Spectroscopy*; Mirabella, F. M., Ed.; John Wiley and Sons, Inc.: New York, 1998, pp 185-217.

(27) Fritz, J. S. *Analytical Solid-Phase Extraction*; John Wiley & Sons: New York, 1999.

(28) Plumlee, D. K. *32nd International Conference on Environmental Systems, San Antonio, TX* 2002, *SAE Technical Paper #2002-01-2537.*

(29) DuPont Oxone Monopersulfate Compound Technical Information, http://www.dupont.com/oxone/techinfo/index.html, 1998.

(30) Howard, S. G.; Hutchens, C. F.; Rethke, D. W.; Swartley, V. L.; Marsh, R. W. *28th International Conference on Environmental Systems, Danvers, MA, USA* 1998, *SAE Technical Paper #981620.*

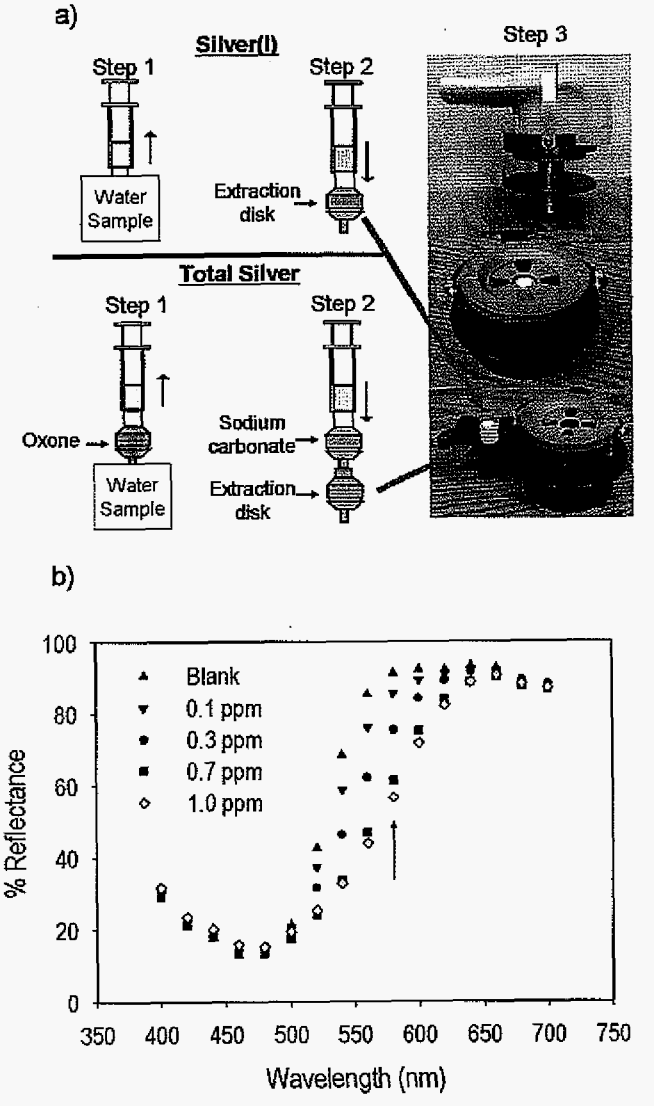

Figure 1. a) Schematic of the procedures for determining silver(I) (top left) and total silver (bottom left) by C-SPE. For both methods, Step 1 is sample collection, Step 2 is analyte extraction, and Step 3 (far right) is membrane interrogation using the handheld DRS instrument with sample holder. b) Representative DR spectra from an analysis of silver(I). The *F(R)* value calculated from the reflectance at 580 nm is used for analyte quantification.

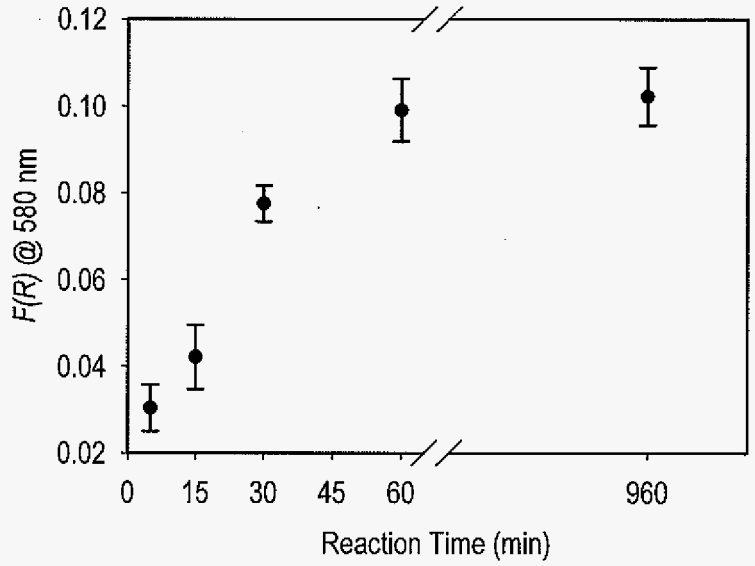

Figure 2. Plot of KM function (n = 3) vs. reaction time for the C-SPE determination of total silver using ~6 mg/mL Oxone as an oxidizing agent and a sample containing 80-nm colloidal silver at a concentration of 0.57 ppm.

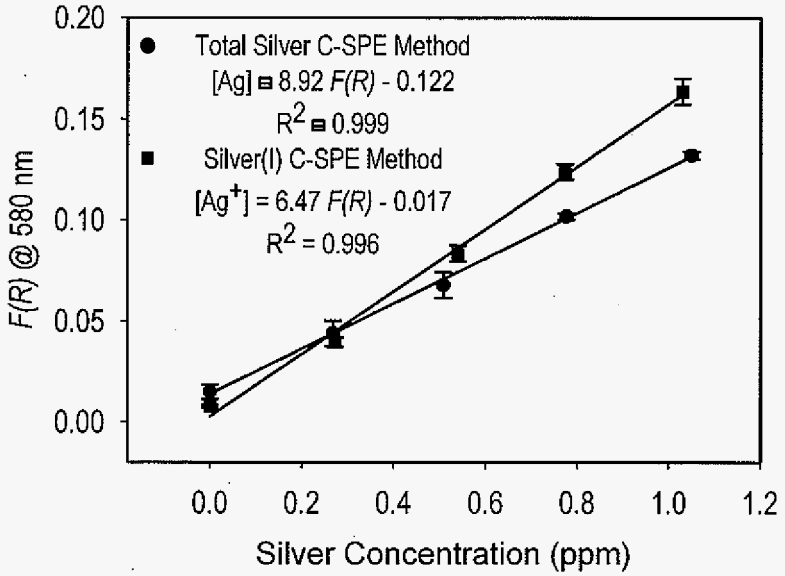

Figure 3. Response of the finalized C-SPE method for total silver, which uses ~25 mg/mL Oxone as an oxidizing agent and sodium carbonate to neutralize the excess Oxone before the extraction step. A calibration plot for the silver(I) C-SPE method is provided for comparison. Each plot was generated by carrying out the corresponding procedure in triplicate on samples prepared by diluting a silver atomic absorption standard.

Table 1. Validation of the C-SPE method for total silver using purchased colloid solutions. The three samples were prepared by mixing equal volumes of the 20, 40, 60, and 80-nm silver colloid solutions (i.e., each particle size accounts for ~25 % of the total silver concentration) and diluting with deionized water.

Colloidal Sample†	Silver Concentration (ppm) by ICP-MS	Silver Concentration (ppm) by C-SPE	% Difference‡
1	0.95 ± 0.05	1.03 ± 0.09	8.7
2	0.42 ± 0.02	0.42 ± 0.01	1.7
3	0.12 ± 0.01	0.124 ± 0.008	0.60

† See Section 4.2 for additional information on sample preparation.

‡See Section 4.2 for an explanation of the trend in percent difference.

Note: The silver(I) C-SPE method detected 10% or less of the silver in each sample.

Table 2. Validation of the C-SPE method for total silver using an ISS potable water sample containing electrolytically-generated silver.

Method	ICP-MS	Total Silver C-SPE	Silver(I) C-SPE	Colloidal Silver*
Silver (ppm)	0.45 ± 0.02	0.45 ± 0.05	0.32 ± 0.03	0.13 ± 0.06

*Colloidal silver concentration calculated by subtracting silver(I) concentration from total silver concentration.

CHAPTER 3. A RAPID, SIMPLE METHOD FOR DETERMINING FORMALDEHYDE IN DRINKING WATER USING COLORIMETRIC-SOLID PHASE EXTRACTION

A paper to be submitted to *Analytica Chimica Acta*

April A. Hill, Robert J. Lipert, James S. Fritz, and Marc D. Porter*†

Iowa State University, Institute for Combinatorial Discovery, Departments of Chemistry and of Chemical and Biological Engineering, and Ames Laboratory-U.S. DOE, Ames, IA 50011-3020

†Department of Chemistry and Chemical Engineering, University of Utah, Salt Lake City, UT 84108

*Corresponding author

Abstract

Formaldehyde has been detected in drinking water supplies across the globe as well as on board NASA spacecraft. A rapid, simple, microgravity-compatible technique for measuring this contaminant in water supplies using colorimetric solid-phase extraction (C-SPE) is described. This method involves collecting a water sample into a syringe by passage through a cartridge that contains sodium hydroxide, to adjust pH, and Purpald, which is a very sensitive and selective colorimetric reagent for aldehydes. After completing the reaction in the syringe by agitating for 2 min on a shaker at 400 rpm, the 1.0-mL alkaline sample is passed through an extraction disk that retains the purple product. The amount of concentrated product is then quantified on-disk using diffuse reflectance spectroscopy. Finally, the formaldehyde concentration is determined via calibration plots generated from Kubelka-Munk transformations of the reflectance data at 700 nm. This method is capable of determining formaldehyde concentrations from

0.08 to 20 ppm with a total work-up time of fewer than 3 min using only 1-mL samples.

1. Introduction

Formaldehyde can be introduced into drinking water by the oxidation of natural organic (humic) matter during water treatment.[1,2] It can also enter drinking water via leaching from polyacetal plastic fittings if the protective coating is breached.[3] Since chronic exposure by ingestion leads to adverse gastrointestinal effects, the EPA has set health advisory levels for formaldehyde in drinking water that range from 10 mg L^{-1} (ppm) for a 1-day exposure to 1 ppm for a lifetime of exposure.[4]

Adding a new dimension to concerns about formaldehyde contamination, trace levels of this hazardous compound have been detected in several water samples collected on International Space Station (ISS).[5] Two major sources of formaldehyde have been identified: (1) off-gassing of polymeric materials, and (2) by-products of metabolic processes. Once present in the air of the spacecraft cabin, formaldehyde can enter the drinking water as humidity condensate, which has been found to contain up to 9 ppm formaldehyde.[6] Therefore, to safeguard crew health, NASA has developed a set of spacecraft water exposure guidelines which limit formaldehyde concentrations to 20 ppm for a 1-10 day exposure and 12 ppm for a 100-1,000 day mission.[6]

Currently, spacecraft drinking water supplies are evaluated using samples collected on ISS and returned to Earth for analysis. This process often results in a gap of several months between sample collection and analysis, which raises sample degradation issues and prevents the timely implementation of correction scenarios. These factors underscore the need for rapid, on-board methods for monitoring trace levels of critical components in spacecraft drinking water supplies. For this purpose, these methods must have sufficient selectivity and sensitivity to detect analytes at low concentrations, and be user-friendly, small, lightweight, and capable of operation in microgravity. As recent reports from our laboratory have shown,[7-11] colorimetric solid-phase extraction (C-SPE) has demonstrated the ability to meet many of these requirements.

C-SPE is a novel sorption-spectrophotometric technique that combines colorimetric chemistry with SPE to determine analyte concentration by measuring the color change of single-use SPE membranes. A hand-held diffuse reflectance spectrophotometer is used to rapidly quantify membrane-bound analytes using the Kubelka-Munk (KM) function.[12,13] The complete procedure typically requires only 1-2 min. The three main variations of C-SPE are: (1) colorimetric complexation followed by product extraction; (2) analyte extraction followed by complexation; and (3) impregnation of colorimetric reagent followed by simultaneous extraction and complexation of the analyte. To date, our laboratory has utilized two of these modalities to develop methods that meet NASA water quality monitoring requirements. Impregnation followed by extraction is the basis for our approaches to

monitor the biocidal agents silver(I) and I_2 as well as the metal contaminants copper(II), iron(III), and chromium(VI).[7,9,14] Complexation and extraction involves colorimetric reagents that are immobilized on inert media and released into samples to form a product that is subsequently collected on an extraction disk. This technique was demonstrated in the determination of nickel(II).[11] We have also employed the concept of immobilized reagents to adjust pH and to oxidize an analyte to a more readily detectable product.[7,11] Notably, the use of reagents that have either been impregnated in the extraction membrane or immobilized on inert media eliminates the need to handle solvents and chemicals throughout sample workup. This approach enables C-SPE to function in a "reagentless" format, thereby minimizing exposure to hazardous materials.

Ongoing research in our laboratory is aimed at developing methods for determining pH and cadmium.[15,16] In addition, efforts are underway to combine several analyses into a multiplexed platform to enhance sample throughput [17] as well as to investigate the possibility of operating in a negligible-depletion regime to eliminate the need for accurate metering of water samples in C-SPE experiments.[18] We have also initiated assessments of the performance of these methods in microgravity,[8,10,19] which have recently shown excellent agreement between KC-135 flight simulations and ground-based analyses of iodine and silver(I).[20]

This work extends the scope of C-SPE by the development of a method that is capable of monitoring formaldehyde concentrations from 0.02 to 20 ppm in aqueous samples using Purpald[21-27] as the colorimetric reagent. Purpald offers

several advantages over other colorimetric reagents (e.g., chromotropic acid, acetylacetone, dinitrophenylhydrazine, etc.)[28,29] employed to detect formaldehyde. A determination using Purpald can be extremely sensitive—as little as 1 nanomole formaldehyde has been detected.[22] Purpald is also very specific—it does not form purple-colored products with ketones, esters, amides, hydrazines, formic acid, and other common interferents in the measurement of aldehydes.[30] In addition, Purpald reacts at room temperature and is stable, thus avoiding the heating step required for the chromotropic acid method and the explosion hazard associated with dinitrophenylhydrazine.[28,29] As illustrated in Scheme 1, Purpald **(I)** combines with formaldehyde in alkaline solution to form a colorless intermediate **(II)**. This intermediate is then oxidized by ambient oxygen to form an intensely purple tetrazine **(III)**,[25] which serves as the colorimetric product.

Commercially available formaldehyde test kits that rely on Purpald suffer from several disadvantages when compared with the method developed herein. First and foremost, none are applicable to a microgravity environment, which is obviously required for in-flight water quality monitoring for NASA missions. These kits, including those manufactured by Merck under the names Spectroquant, Aquamerck, Reflectoquant, and Merckoquant, are unsuitable for use in microgravity based on factors such as (1) the necessity of adding drops of concentrated sodium hydroxide into liquid samples, (2) the need to dip a reagent strip into liquid samples and allow excess liquid to drip off, or (3) the need to dilute samples with deionized water to cover the range of interest. Due to the difficulties with fluid handling caused by

reduced gravity, such testing methodologies would have to be modified greatly in order to be useful for in-flight water quality monitoring. Also, the added hazards and costs associated with the transport and storage of the concentrated sodium hydroxide solution is a significant drawback to carrying such kits on shuttle missions. In addition, most of these kits are only semi-quantitative and, as such, are unable to accurately determine formaldehyde concentrations in NASA's target range for potable water.

The following sections detail the development of a C-SPE method that uses immobilized forms of Purpald and sodium hydroxide, both of which are loaded into a filter holder that serves as the "reagent cartridge". The procedure involves collecting a water sample into a 3-mL syringe by passage through the reagent cartridge. The air (~1 mL) that occupies the dead volume of the cartridge is also drawn into the syringe, providing a source of oxygen for the oxidation step in Scheme 1. Experiments were also carried out to assess the use of oxidizing agents (i.e. Oxone and hydrogen peroxide) or sample agitation as a means to speed the slow air-oxidation step. We determined that agitating the sample on a shaker significantly decreased the reaction time with air oxidation to only ~2 min. These findings, when optimally integrated, yield a method capable of detecting formaldehyde in the range of 0.08 to 20 ppm in less than 3 min. The developed method is not only ideal for application to NASA's water quality monitoring needs, but is also more user-friendly, provides better quantitation with a lower detection limit, requires smaller samples,

and is less hazardous to the user when compared to existing test kits for monitoring formaldehyde in Earth-bound applications.

2. Experimental

2.1 Reagents and chemicals

All solutions were prepared daily with deionized water that was purified by a Millipore Milli-Q water purification system. The oxidizing agents Oxone and hydrogen peroxide (H_2O_2, 30% (v/v)) were obtained from Aldrich.

2.1.1 Formaldehyde sample solutions

Solutions with formaldehyde concentrations up to 20 ppm were prepared in Nalgene bottles by diluting the appropriate mass of a formalin solution (37% (wt) formaldehyde, Sigma-Aldrich) with either deionized water or 0.50 M sodium hydroxide in deionized water.

2.1.2 Purpald reagent solution

A Purpald reagent solution was prepared by dissolving 0.10 g Purpald (Aldrich) in 10.0 mL of 0.50 M sodium hydroxide in deionized water.

2.1.3 Extraction cartridges

Empore™ Anion Exchange-SR 47-mm extraction membranes (3M) were used as received to collect the colorimetric complex. The membranes were cut into 13-mm disks to fit into Swinnex polypropylene filter holders (Fisher). The disks were

placed on top of the support screen located in the bottom portion of the holder. The holder was then assembled by sealing against a silicone gasket.

2.1.4 Reagent cartridges

A 2.0-mL aliquot of 6.0 M NaOH was poured over a 45-mm diameter Millipore Media Pad (Fisher) that was placed in a 50-mm glass Petri dish. Once saturated with liquid, the pad was cut into 10-mm disks and dried gently on a hot plate for ~12 h. When dry, each disk was mounted in place of the support screen in the bottom of a Swinnex holder.

Purpald immobilization was accomplished by loading a 13-mm diameter disk, cut from Whatman #1 filter paper, into the top portion of a Swinnex holder (with gasket) and placing 6 mg of the reagent onto the center of the disk. A second filter paper disk was used to cover the reagent and the top and bottom (containing the NaOH disk) portions of the holder were then mated. This step secured the reagent between the two filter paper disks.

2.2 Instrumentation and Software

Sample agitation experiments were carried out using either a BI model 4630 3-D rotator or a NBS model C24 benchtop shaker. All transmission spectra were collected using a Hewlett-Packard model 8453 UV-Vis spectrophotometer. The sample holders were quartz cuvettes with a 1.00-cm pathlength. A BYK-Gardner color-guide sphere (d/8°) diffuse reflectance spectrophotometer (Model LCB-6830) was employed to measure the diffuse reflectance spectra (DRS) of the disks after

extraction of the colored product. This hand-held spectrophotometer is small, lightweight, battery-operated, and can acquire reflectance data in under 2 s over the visible spectral range (400-700 nm) at 20-nm intervals.[10] Once collected, the DRS are downloaded to a personal computer and analyzed using BYK-Gardner QC-Link software that was modified in-house to calculate the Kubelka-Munk (KM) function (*F(R)*).[12] The KM function is given by Equation 1,

$$F(R) = (1 - R)^2 / 2R \quad (1)$$

where R is the diffuse reflectance of the sample relative to a reflectance standard. We note that *F(R)* is directly related to the concentration of the complex in the membrane, C, by Equation 2,

$$F(R) = 2.303\varepsilon C / s \quad (2)$$

where ε is the molar absorptivity of the colorimetric product and s is the scattering coefficient of the sample surface. The solution concentration of the analyte is determined by means of a calibration plot of *F(R)* at a given wavelength versus analyte concentration.

3. Method Development

Preliminary experiments were carried out to assess if Purpald was a viable reagent for the development of a C-SPE method for determining formaldehyde. These tests were designed to address: (1) whether the product could be retained on an SPE disk; and (2) whether the DRS of the disk could be correlated to

formaldehyde concentration. A study was also conducted to determine the possibility of adding an oxidizing agent to the system to increase the rate of formation of III, the purple tetrazine product.

3.1 Extraction and quantification of the air-oxidized product

As a starting point, the reaction was carried out using a method adapted from Dickinson and Jacobsen,[31] in which 10.0 mL of formaldehyde solutions (0.50 M NaOH) of varied concentrations were added to 10.0 mL of Purpald solutions in a 25.0-mL volumetric flask. Upon completion of the two-step reaction (~35 min), the sample was diluted to the mark with 0.5 M NaOH. A 1.0-mL sample of each solution was then collected in a 3-mL, polypropylene syringe (HSW Norm-Ject®) and passed through an extraction cartridge to collect the product on the disk. After extraction, the holder was separated from the syringe and the sample disk was dried by passage of ~60 mL of air using a 60-mL syringe. The sample holder was then opened and the lower portion was mounted on the sample locator of the spectrophotometer for interrogation.

Figure 1a presents the DRS obtained from the analysis of formaldehyde between 0.10 and 0.95 ppm. A spectrum for a blank solution (i.e., Purpald in 0.5 M NaOH) is also presented. Though literature reports the absorbance maximum of the product in solution at 549 nm,[31] the maximum of the Kubelka-Munk function (minimum reflectance) for the on-membrane analysis occurs at ~560 nm. Figure 1a clearly shows, however, that solutions with formaldehyde concentrations above ~0.5 ppm cannot be distinguished at this wavelength. An examination of the

response at each wavelength revealed that 700 nm was the most effective analytical wavelength; that is, the calibration plot at 700 nm, given in Figure 1b, exhibited the most linear profile. Moreover, this wavelength yielded a level of performance which surpassed that specified by both EPA and NASA.[4,6] Using the standard deviation of the blank determined from three measurements and the equation of the regression line, the limit of detection (LOD) for formaldehyde was calculated to be ~50 ppb.

3.2 Effect of additional oxidizing agent on reaction rate

The effect of adding an oxidizing agent to the system was investigated in an attempt to reduce the time required for the second step of the colorimetric reaction. Previously, our laboratory developed a C-SPE method for detecting iodide in water via the oxidizing agent Oxone, which converts iodide to iodine, and the subsequent extraction of iodine onto a membrane impregnated with poly(vinylpyrrolidone).[7] Oxone was employed because of its oxidizing power, stability in powder form, and solubility in water at neutral pH. However, Oxone was found to be largely insoluble in the alkaline solution required for the Purpald reaction, and did not have a detectable effect on the rate of oxidation.

An earlier report has shown that H_2O_2 is an effective oxidizing agent for this reaction.[24] To test the merits of this possibility, UV-Vis spectroscopy was used to compare the rate of product formation when H_2O_2 was added to the system to that for air oxidation. The air-oxidation experiment was carried out by rapidly mixing 50.0 mL of 10.0 ppm formaldehyde (0.5 M NaOH) and 50.0 mL of Purpald solution in

a flask and periodically withdrawing a sample for spectrophotometric characterization.

The procedure for peroxide oxidation was almost identical to that for air oxidation. However, upon visual observation of the first trace of purple color, which indicated the onset of the oxidation step, 1.7 mL of H_2O_2 (see below) were added to the flask, and the spectrum of the product was again monitored as a function of time. No detectable color development occurred when H_2O_2 was added before the onset of any observable air-induced oxidation, indicating that peroxide oxidation of the starting reagents altered their reactivity.

A plot of the absorbance at 550 nm as a function of time after mixing reagents revealed that the reaction with ambient air reaches completion in ~20 min. The addition of H_2O_2, however, decreased this time to ~10 min. This result points to the preferential usage of H_2O_2 as an oxidizing agent. However, the absorbance for the H_2O_2–oxidized product was lower than that for air oxidation. Spectral analysis revealed that the lower absorbance results from a shift in the absorbance maximum of the product in the H_2O_2 reaction scheme toward shorter wavelengths. Interestingly, the addition of more than 1.7 mL of H_2O_2 caused the rapid (<10 s) formation of a bright red product. The UV-Vis spectrum of this product had two maxima, 500 and 315 nm. We believe this change results from the coupling of **III** via disulfide linkages,[32-35] which reduces the delocalization of π-electron density and shifts the absorbance of the new material to shorter wavelengths. If this is the case,

the signal generated by the red product should also be proportional to formaldehyde concentration. The next section investigates this possibility.

3.3 Extraction and quantification of the peroxide-oxidized product

To determine whether the red product created by oxidation with excess H_2O_2 could be used to quantify formaldehyde, a calibration experiment was carried out. The previously described solution-based calibration procedure was used, but with the addition of 2.0 mL of H_2O_2 immediately after the appearance of a purple color, which signaled the onset of the oxidation step. The solutions, which rapidly turned to various shades of red, were agitated on a stir plate for 35 min to remove the gas bubbles generated by H_2O_2. The solutions were then brought up to the 25.0-mL mark with 0.5 M NaOH, and three 1.0-mL samples from each solution were analyzed by C-SPE.

Like the UV-Vis data mentioned in Section 3.2, the reflectance spectra shown in Figure 2a indicate that the wavelength of maximum absorbance for the red-colored product is ~500 nm. As with the purple product, the KM function at 500 nm proved to be too strong over the targeted concentration range, so the calibration plot in Figure 2b was generated using the data at 460 nm. This plot shows a clear linear trend and has a LOD about four times lower than that for the purple product. Although the time saved by rapid oxidation is somewhat offset by the need for bubble removal, this finding suggests the H_2O_2–based method has obvious merits for analysis of samples on Earth. However, the preferred embodiment for spaceflight applications is a "reagentless" system in which all requisite reagents are immobilized

onto inert media. As a consequence, and in view of our focus on providing microgravity-compatible methods, no further studies with H_2O_2 were conducted.

4. Results and Discussion

To meet the objective of creating a "reagentless" method for quantifying formaldehyde, the requisite reagents were immobilized onto inert media and loaded in the reagent cartridge as previously described. The reagent cartridges were connected to 3-mL Luer Lock polypropylene syringes and aqueous solutions of formaldehyde were drawn into the syringes through the cartridges. During collection, the liquid sample first passes through the NaOH disk, which raises the pH above 10, facilitating the dissolution of the immobilized Purpald. In addition to the liquid sample, the air (~1 mL) that occupies the dead volume of the holder is drawn into the syringe, providing a source of oxygen for formation of the purple product. When filled, the 3-mL syringes contain ~1 mL of air and ~2 mL of sample solution. Once the reaction is complete, the air and excess liquid are expelled and the remaining 1.0-mL reacted sample is forced through the extraction cartridge. Finally, the membrane is dried by passage of ~60 mL of air, the holder is disassembled, and the spectrum of the disk is acquired.

4.1 Two-hour calibration using rotator

Preliminary results with the reagent cartridges indicated that the time required for air oxidation could be reduced by agitating the contents of the syringe, which increases the rate of purple product formation. Immediately after sample collection,

the syringes were capped and placed on a 3-D rotator at a setting of 30 rpm. It was experimentally determined that the *F(R)* value at the analytical wavelength (700 nm) reached a stable maximum after about 1.5 h of rotation. Thus, the calibration plots presented in Figure 3 were obtained from four samples at each concentration after 2 h of rotation. Figure 3a shows the results of an analysis of formaldehyde concentrations up to 1 ppm, which yields a calculated limit of detection (LOD) of ~60 ppb.

The response over the full range targeted by NASA and EPA (i.e., up to 20 ppm) is shown in Figure 3b. The deviation from linearity at the upper range of this plot can be explained by examining the reflectance data. For formaldehyde concentrations above ~10 ppm, the disk is extremely dark, leading to exceedingly low reflectance values (i.e., less than 0.2). These reflectance values fall in the high error regime for *F(R)* analyses ($0.2>R>0.7$).[13]

As mentioned earlier, the maximum of the KM function occurs at 560 nm, but the strength of the signal at this wavelength prevented quantification of formaldehyde concentrations above ~0.5 ppm. However, the use of 560 nm should result in the ability to quantify formaldehyde at concentrations below the LOD achieved at 700 nm. To test this hypothesis, the analysis was performed on aqueous formaldehyde samples with concentrations between 10 and 60 ppb using the more sensitive wavelength. Analysis of the results indicated that better linearity and reproducibility in the calibration data could be achieved using 540 nm rather than 560 nm as the analytical wavelength. Therefore, the *F(R)* at 540 nm was used to

create the calibration plot in Figure 4. Clearly, by using a more sensitive wavelength, the utility of this method has been expanded to cover even lower levels of formaldehyde, decreasing the LOD to 20 ppb.

4.2 Two-minute calibration using shaker

In an attempt to further reduce reaction time, a shaker with a maximum speed of 400 rpm was used in place of the rotator. As expected, the oxidation rate was greatly increased in comparison to that achieved using the rotator. After as little as 1 min at 400 rpm (in addition to the 1 min required for the shaker to reach 400 rpm), there was sufficient color development to facilitate the generation of a calibration plot from the KM function of the extraction disks at 700 nm. The procedure for this method involved filling, capping, and placing the syringe on the shaker for 1 min at 400 rpm (2 min total). After shaking, the air and excess sample volume were expelled and the remaining 1.0-mL sample was passed through the extraction cartridge.

The calibration plot obtained for solutions with formaldehyde concentrations between 0.25 and 1.0 ppm, shown in Figure 5a, yields a calculated LOD of 80 ppb. Figure 5b, in contrast, summarizes the response for formaldehyde concentrations up to 20 ppm. The decrease in sensitivity and measurement precision compared with that of the rotator experiments are explained by the fact that the air oxidation step is not complete after shaking. Rather, it has been accelerated for a given time and then the reaction terminated before oxidation is complete, leading to a decrease in signal. Moreover, with such a short reaction interval, small variations in the time between

filling the syringe and passing the sample through the extraction membrane can contribute significantly to the deviation in the data. However, the data clearly show that this method has the capability to determine formaldehyde concentrations as low as 80 ppb in less than 3 min.

Notably, the slope of the plot for the higher concentration range is approximately twice that for the lower range. Similar trends are observed with several C-SPE methods, and we believe this phenomenon is related to the diffuse reflectance measurements rather than the colorimetric chemistries involved. This conclusion was supported by an experiment in which dilutions of **III** were prepared after carrying out Scheme 1 on a concentrated solution of formaldehyde. Though Equation 2 indicates that the C-SPE response for such dilutions should follow a linear trend, the experimental data revealed increased sensitivity at higher concentrations. We attribute this change to the fact that, for strongly absorbing analytes such as **III**, one of the assumptions involved in KM theory is not valid; i.e., that the sampling depth remains constant as the concentration of the absorbing species changes. In reality, as the amount of **III** in the membrane increases, more of the incident light is absorbed by the colorimetric product collecting in the upper layers of the membrane. Though negligible at low concentrations of **III**, this trend eventually leads to a detectable decrease in beam penetration depth, which in turn decreases the volume of membrane sampled by the incident light. Consequently, as the formaldehyde concentration continues to increase, the apparent concentration of

III in the membrane increases not only because more **III** is produced and extracted, but also because the volume of membrane sampled is decreasing.

Attempts to calibrate the response of the shaker method at the low ppb range using 540 nm as the analytical wavelength were unsuccessful due to very low signal-to-noise ratios in the data. We attribute this to two factors: (1) the variability in time between filling and measuring each sample, and (2) the high levels of reflectance (low *F(R)* values) obtained for these disks, which fall in the high-error regime for *F(R)* analyses.

4.3 Interference study

A study was carried out to determine the effects of potential interferents on this analysis. Acetaldehyde and propionaldehyde, being the next two compounds in a homologous series, were tested. Benzaldehyde was included to determine the effect of aromaticity. Finally, ethylene glycol was examined since it is readily oxidized to formaldehyde.[36] Moreover, the first three substances have been detected, albeit at low (<8 ppb) levels, in spacecraft water supplies; ethylene glycol, in contrast, has been detected at levels as high as 1 ppm.[5]

The impact of each interferent was examined by generating two sample solutions: one containing a 1:1 ratio of interferent to formaldehyde, and the other a 10:1 ratio. The 1:1 samples consisted of ~5 ppm of the interferent and ~5 ppm formaldehyde, while the 10:1 samples were composed of ~5 ppm interferent and ~0.5 ppm formaldehyde. Each solution was tested four times with both rotator and

shaker agitation, and the average *F(R)* at 700 nm was compared to that predicted by the calibration equation for the given concentration of formaldehyde in each solution. Although shaker agitation is the preferred method for rapid formaldehyde detection, rotator agitation is potentially useful for determining low ppb levels of formaldehyde, so interference tests were carried out using both methods.

4.3.1 Rotator interference study

The responses obtained from the rotator interference tests are shown in Figure 6, along with the calibration plot obtained for formaldehyde. Though all of the aldehydes tested are potential interferents in the determination of formaldehyde by Purpald, literature has shown that structural differences in the products formed by different aldehydes lead to variations in their spectra.[30,37] Our findings are consistent with the past work. Acetaldehyde, which differs by only one methyl group, is the strongest interferent, producing a signal that would be interpreted as a false positive in the absence of formaldehyde. However, the addition of another methyl group, creating propionaldehyde, or the substitution of an aromatic ring, producing benzaldehyde, causes a decrease in the interfering signal. Ethylene glycol was the only species found to have no effect on the determination of formaldehyde by this method. Presumably, at the conditions of the reaction, ethylene glycol is not detectably oxidized to formaldehyde.

4.3.2 Shaker interference study

As previously discussed, the colorimetric reaction shown in Scheme 1 does not reach completion when using the shaker method. As a result, the interference

study obtained using the shaker, shown in Figure 7, exhibits some interesting differences from that of the rotator. The lack of detectable interference from ethylene glycol is consistent with the results obtained in the rotator trials. Similarly, the response of acetaldehyde appears to be decreased to the same relative degree as that of formaldehyde. Consequently, acetaldehyde interferes to the same degree as in the rotator method. However, the larger aldehydes exhibit a greater reduction in signal than formaldehyde, and thereby interfere to a lesser degree. This observation can be explained by examining the reaction mechanism shown in Scheme 1. Past work has shown that larger aldehydes react more slowly with Purpald, a fact which is attributed to a sterically induced decrease in the rate of formation of **II**.[38] This decrease in intermediate formation causes a delay in the onset of the oxidation step. In this experiment, though the rapid shaking of the syringe increases the rate of the oxidation step, it has no effect on the rate of the initial reaction between Purpald and the aldehyde, which is limited by steric constraints. Therefore, the rate of formation of the purple product with more hindered aldehydes is not as greatly increased by shaking as that for the less bulky aldehydes, resulting in a decreased level of interference from the larger aldehydes.

5. Conclusions

This work details the successful development of a C-SPE method for the rapid (~3 min) quantification of aqueous formaldehyde from 0.08 to 20 ppm using only a 1.0-mL sample volume. Covering this broad concentration range with such a small sample is extremely useful on board spacecraft, where there is a limited

supply of potable water. In addition to its microgravity compatibility, the C-SPE method is more user-friendly, provides better quantitation, has a lower detection limit, requires smaller samples, and is less hazardous to the user than existing formaldehyde test kits. These advantages make the C-SPE method attractive for use in many ground-based applications as well. This method could, for instance, be implemented in the water treatment industry as a low-cost, rapid, simple option for monitoring water quality during treatment processes known to produce formaldehyde as a byproduct. One major advantage is that C-SPE methods are amenable to packaging into a kit for monitoring water quality in underdeveloped regions where analytical services are not available and contamination is a serious risk. In order to produce such a kit for use in both ground and flight analyses of potable water, we plan to continue to expand the utility of C-SPE to cover an even broader range of analytes that affect human health. To this end, future work with the current method will focus on expanding its usefulness to the detection of glycols, which are introduced into spacecraft water supplies through the use of no-rinse personal hygiene products.

Acknowledgements

The authors would like to thank Jeff Rutz, Dan Gazda and John Schultz of Wyle Laboratories, Houston, TX, USA for their insightful discussions. This work was supported by NASA contract NAG91510. The Ames Laboratory is operated by Iowa State University under U.S. Department of Energy contract DE-AC02-07CH11358.

References

(1) Becher, G.; Ovrum, N. M.; Christman, R. F. *Sci. Total Environ.* **1992**, *117-118*, 509-520.

(2) Glaze, W. H.; Koga, M.; Cancilla, D. *Environ. Sci. Technol.* **1989**, *23*, 838-847.

(3) IPCS *Concise International Chemical Assessment Document No. 40*; World Health Organization, Geneva, 2002.

(4) Toxicological Profile for Formaldehyde, http://www.atsdr.cdc.gov/toxprofiles/tp111.html, 1999.

(5) Plumlee, D. K. *32nd International Conference on Environmental Systems, San Antonio, TX* **2002**, *SAE Technical Paper #2002-01-2537.*

(6) McCoy, J. T. In *Spacecraft Water Exposure Guidelines for Selected Contaminants: Volume 2*; National Academies Press, 2006; Vol. http://www.nap.edu/catalog/11778.html, pp 301-342.

(7) Arena, M. P.; Porter, M. D.; Fritz, J. S. *Anal. Chem.* **2002**, *74*, 185-190.

(8) Arena, M. P.; Porter, M. D.; Fritz, J. S.; Mudgett, P.; Rutz, J.; Schultz, J. *32nd International Conference on Environmental Systems, San Antonio, TX* **2002**, *SAE Technical Paper #2002-01-2535.*

(9) Arena, M. P.; Porter, M. D.; Fritz, J. S. *Anal. Chim. Acta* **2003**, *482*, 197-207.

(10) Gazda, D. B.; Lipert, R. J.; Fritz, J. S.; Porter, M. D.; Rutz, J.; Mudgett, P.; Schultz, J. *33rd International Conference on Environmental Systems, Vancouver, B.C., Canada* **2003**, *SAE Technical Paper #2003-01-2406.*

(11) Gazda, D. B.; Fritz, J. S.; Porter, M. D. *Anal. Chim. Acta* **2004**, *508*, 53-59.

(12) Kortum, G. *Reflectance Spectroscopy: Principles, Methods, Applications*; Springer: New York, 1969.

(13) Blitz, J. P. In *Modern Techniques in Applied Molecular Spectroscopy*; Mirabella, F. M., Ed.; John Wiley and Sons, Inc.: New York, 1998, pp 185-217.

(14) Fritz, J. S.; Arena, M. P.; Steiner, S. A.; Porter, M. D. *J Chromatogr. A* **2003**, *997*, 41-50.

(15) Shih, C. J.; Dias, N. C.; Porter, M. D. *35th International Conference on Environmental Systems, Rome, Italy* **2005**, *SAE Technical Paper #2005-01-2890.*

(16) Nordling, J.; Lipert, R. J.; Porter, M. D.; Gazda, D. B. *35th International Conference on Environmental Systems, Rome, Italy* **2005**, *SAE Technical Paper #2005-01-2891.*

(17) Gazda, D. B.; Fritz, J. S.; Porter, M. D. *Anal. Chem.* **2004**, *76*, 4881-4887.

(18) Dias, N. C.; Fritz, J. S.; Porter, M. D. *35th International Conference on Environmental Systems, Rome, Italy* **2005**, *SAE Technical Paper #2005-01-3065.*

(19) Ponton, L. M.; Gazda, D. B.; Lipert, R. J.; Fritz, J. S.; Porter, M. D.; Rutz, J.; Mudgett, P.; Dungan, D.; Schultz, J. *33rd International Conference on Environmental Systems, Vancouver, B.C., Canada* **2003**, *SAE Technical Paper #2003-01-2408.*

(20) Porter, M. D.; McCoy, J. T.; Hazen-Bosveld, A. A.; Lipert, R. J.; Nordling, J.; Shih, C. J.; Gazda, D. B.; Rutz, J.; Straub, J.; Schultz, J.; Alverson, J.; Colorimetric Solid Phase Extraction Measurements of Spacecraft Drinking Water Contaminants in: *C-9 Postflight Report*, 2006.

(21) Zurek, G.; Karst, U. *Anal. Chim. Acta* **1997**, *351*, 247-257.

(22) Quesenberry, M. S.; Lee, Y. C. *Anal. Biochem.* **1996**, *234*, 50-55.

(23) Lambert, J. L.; Paukstelis, J. V.; Liaw, Y. L.; Chiang, Y. C. *Anal. Lett.* **1984**, *17*, 1987-1999.

(24) Del Nozal, M. J.; Bernal, J. L.; Hernandez, V.; Toribio, L.; Mendez, R. *J. Liq. Chromatogr.* **1993**, *16*, 1105-1116.

(25) Dickinson, R. G.; Jacobsen, N. W. *Chem. Commun.* **1970**, 1719.

(26) Dickinson, R. G.; Jacobsen, N. W. *Org. Prep. Proced. Int.* **1974**, *6*, 156-157.

(27) Dickinson, R. G.; Jacobsen, N. W. *Anal. Chem.* **1974**, *46*, 298-299.

(28) Pickard, A. D.; Clark, E. R. *Talanta* **1984**, *31*, 763-771.

(29) Goilob, L.; Wellons, J. D. *Forest Prod. J.* **1980**, *30*, 27-35.

(30) Hopps, H. B. *Aldrichimica Acta* **2000**, *33*, 28-30.

(31) Jacobsen, N. W.; Dickinson, R. G. *Anal. Chem.* **1974**, *46*, 298-299.

(32) Zheng, M.; Aslund, F.; Storz, G. *Science* **1998**, *279*, 1718-1721.

(33) Sluis-Cremer, N.; Naidoo, N.; Dirr, H. *Eur. J. Biochem.* **1996**, *242*, 301-307.

(34) Sidorova, M. V.; Molokoedov, A. S.; Az'muko, A. A.; Kudryavtseva, E. V.; Krause, E.; Ovchinnikov, M. V.; Bespalova, Z. D. *Russ. J. Bioorg. Chem.* **2004**, *30*, 101-110.

(35) Aslund, F.; Zheng, M.; Beckwith, J.; Storz, G. *Proc. Natl. Acad. Sci. U. S. A.* **1999**, *96*, 6161-6165.

(36) Hess, E. R.; Jordan, C. B.; Ross, H. K. *Anal. Chem.* **1956**, *28*, 134-135.

(37) Avigad, G. *Anal. Biochem.* **1983**, *134*, 499-504.

(38) *Aldrich Technical Information Bulletin No. AL-145*; Aldrich Chemical Co., Inc.: Milwaukee, WI, 1993.

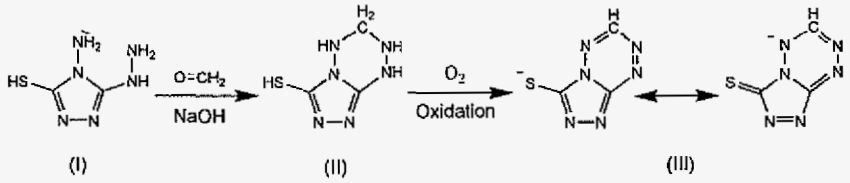

Scheme 1. The reaction of Purpald **(I)** with formaldehyde in alkaline solution. The first step yields a cyclic aminal **(II)**, which is then oxidized in the second step to form a purple tetrazine **(III)**, which exists as an anionic resonance structure in alkaline solution.

a)

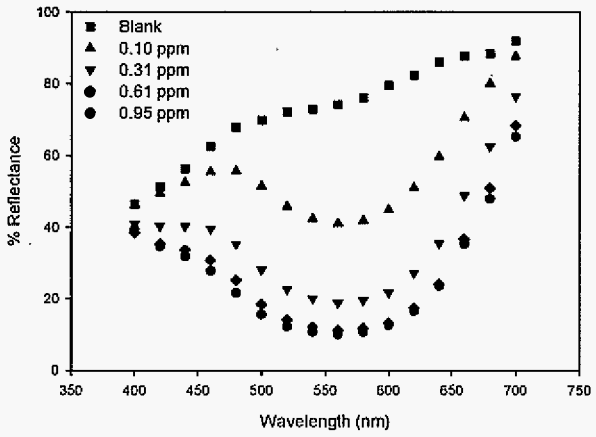

b)

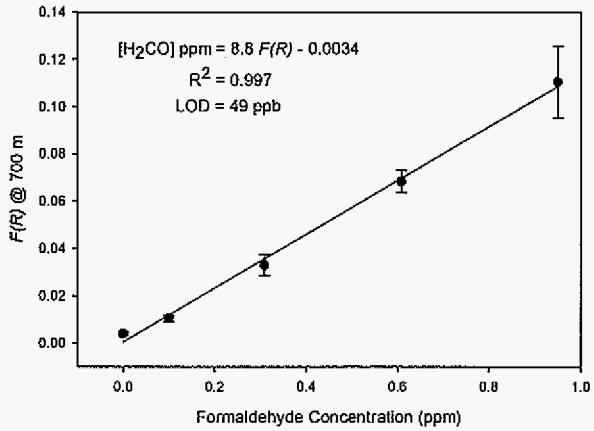

Figure 1. a) DRS of disks used to extract the purple product from 1.0-mL samples and b) calibration plot generated from Kubelka-Munk data at 700 nm.

a)

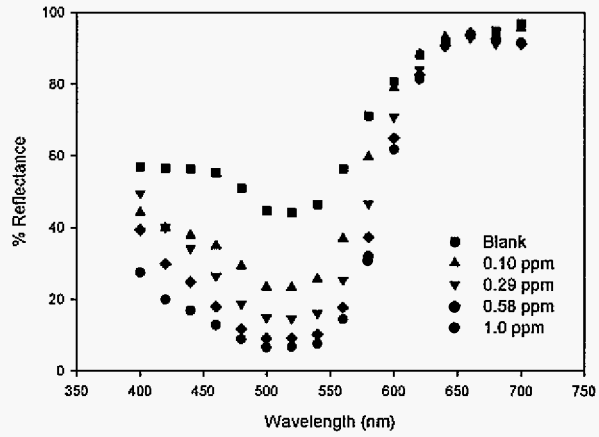

b)

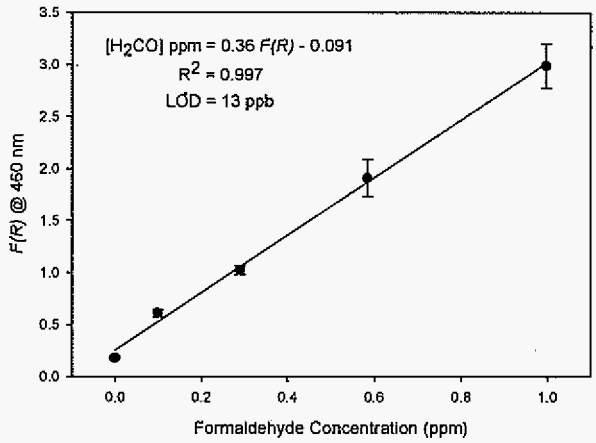

Figure 2. a) DRS of disks after extraction of the red product from 1.0-mL samples of the peroxide-oxidized solutions, and b) calibration plot generated from Kubelka-Munk data at 460 nm.

a)

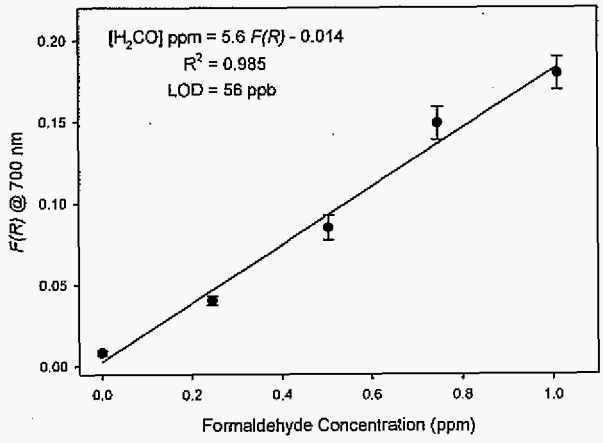

b)

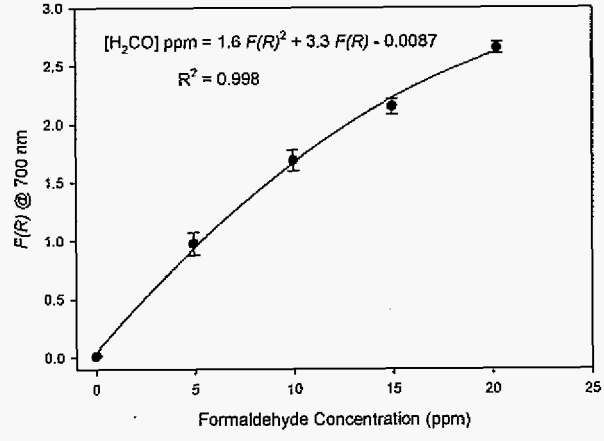

Figure 3. C-SPE response for a) 0.25 to 1.0 ppm formaldehyde and b) 4.9 to 20 ppm formaldehyde after reacting for 2 h on the rotator.

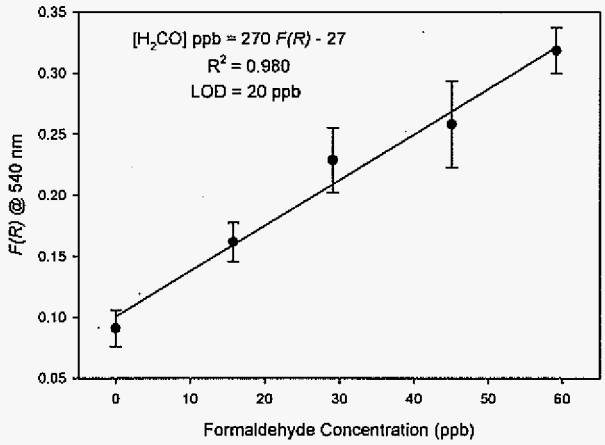

Figure 4. C-SPE response for formaldehyde concentrations up to 60 ppb after reacting for 2 h on the rotator.

a)

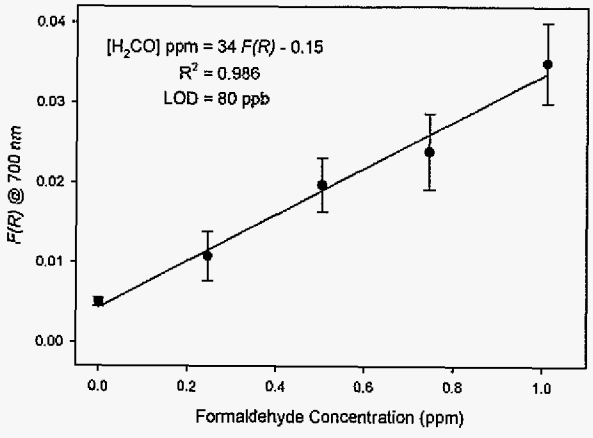

b)

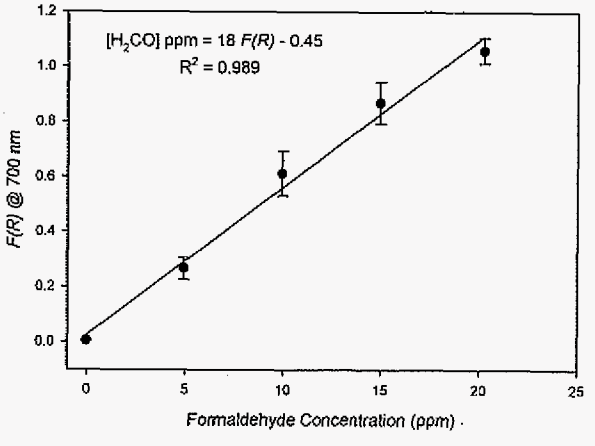

Figure 5. C-SPE response for a) 0.25 to 1.0 ppm formaldehyde and b) 4.9 to 20 ppm formaldehyde after reacting for 2 min on the shaker.

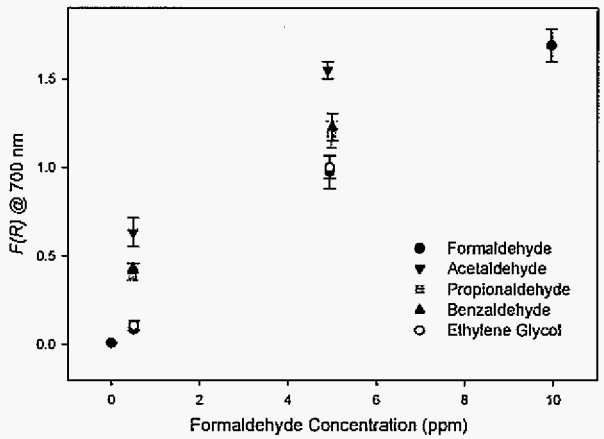

Figure 6. Results obtained from the interference studies performed using the rotator. The *F(R)* for each solution is plotted against the formaldehyde concentration present in that solution. Each interferent solution contained ~5 ppm of the interferent and either ~5 or ~0.5 ppm formaldehyde.

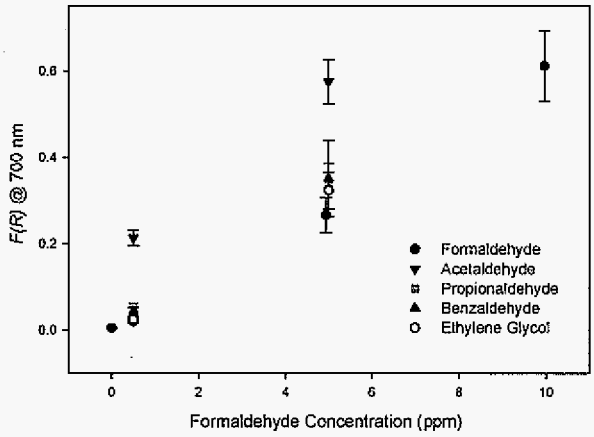

Figure 7. Results obtained from the interference studies performed using the shaker. The *F(R)* for each solution is plotted against the formaldehyde concentration present in that solution. Each interferent solution contained ~5 ppm of the interferent and either ~5 or ~0.5 ppm formaldehyde.

CHAPTER 4. INVESTIGATING THE KINETICS OF HETEROGENEOUS IMMUNOASSAYS USING ROTATED CAPTURE SUBSTRATES

A paper to be submitted to *Analytical Chemistry*

April A. Hill, Gufeng Wang, Robert J. Lipert* and Marc D. Porter*†

Iowa State University, Institute for Combinatorial Discovery, Departments of Chemistry and of Chemical and Biological Engineering, and Ames Laboratory-U.S. DOE, Ames, IA 50011-3020

†Department of Chemistry and Chemical Engineering, University of Utah, Salt Lake City, UT 84108

*Corresponding authors

Abstract

A systematic examination of sandwich-type immunoassay kinetics has been carried out using substrate rotation for control of mass transfer and surface-enhanced Raman scattering (SERS) as a readout modality. Heterogeneous immunoassays often rely on diffusion-limited mass transfer to deliver both the antigen and labeled antibody to the solid capture substrate, which typically translates to long incubation times for both binding steps because the large size of the analytes (e.g., proteins, viruses, and bacteria) and labels (e.g., tagged antibodies) results in comparatively small diffusion coefficients (i.e., slow rates of diffusional transfer). We recently introduced capture substrate rotation as a means to enhance sample and label flux, thereby decreasing assay times from 24 h to 25 min. In addition, the rotation assay had a significantly lower limit of detection (~1 ng/mL) than the assay that used stagnant incubation (~10 ng/mL). Building on these findings, the current work is aimed at a detailed investigation of the effect of substrate rotation on signal

development in sandwich-type immunoassays. Specifically, we examined the effect of rotation on the rate of antigen and label (both specific and nonspecific) binding in a SERS sandwich assay for mouse IgG. This assay used gold nanoparticles coated with both a Raman reporter molecule for detection and an antibody for biorecognition. The findings presented herein indicate that the use of substrate rotation increases the rate of capture of both the antigen and the label in SERS-based immunoassays but has no effect on the rate of nonspecific binding, resulting in assays with shorter incubation times (i.e., 25 min vs 16 h) and signal-to-background ratios that are increased by a factor of ~3.5.

1. Introduction

The immunoassay is an extremely important analytical tool, with applications ranging from human and veterinary medicine to homeland security.[1-4] Currently, immunoassays employ a wide range of readout techniques, including atomic force microscopy (AFM),[5-8], scanning electron microscopy,[9,10] fluorescence-based labeling,[11] and antibody-modified microcantilevers.[12] Though their effectiveness has been aptly demonstrated, these techniques still suffer from various disadvantages. Fluorescence-based immunoassays, for example, suffer from photobleaching and background fluorescence while microcantilevers are extremely fragile and difficult to fabricate.

Recent reports from our laboratory have shown that surface-enhanced Raman scattering (SERS) can be used as a sensitive readout technique for immunoassays.[13-19] The method employs extrinsic Raman labels (ERLs), which

consist of gold nanoparticles that are modified with both an intrinsically strong Raman scatterer and an antibody. The former takes advantage of the well-established enhancement of the Raman scatterering that occurs when the scatterer is coated on nanometer-sized gold particles,[20] and the latter gives the label specificity for the target analyte. We have demonstrated both the sensitivity and the selectivity of this type of immunoassay by the detection of low levels (~30 fM detection limit) of prostate-specific antigen in human serum samples.[15] We have also shown that this method can detect single-digit binding events in the absence of nonspecific adsorption.[19]

In addition to its sensitivity, SERS has several more potential advantages when compared to other readout modalities, particularly with respect to functioning as a multiplexed readout technique. Since the optimum SERS excitation wavelength is dependent on the properties of the enhancing substrate (i.e., the nanoparticle) and not those of the scatterer, multi-label readout can be accomplished with only one excitation wavelength. In addition, Raman bands are much narrower and the response is much less susceptible to photobleaching than fluorescence, enabling the use of extended signal averaging to lower detection limits.

Nonetheless, all heterogeneous immunoassays, including those based on SERS, have a major drawback in that the delivery of an antigen to the solid capture substrate often relies on diffusional mass transport. As a consequence, long incubation times may be necessary because large biological targets (e.g., proteins, viruses, and bacteria) have small diffusion coefficients.[21] This time constraint is even

more problematic for sandwich-type assays since a second incubation step is required for labeling with a tagged antibody.

Several approaches have been investigated to increase the flux of the antigen and label to the capture surface, thereby reducing incubation times. These techniques make use of the fact that antibody-antigen binding is often limited by mass transport rather than by binding kinetics.[22-26] Electric fields, for example, have been used to drive the transport of charged species, reducing the binding time for both DNA hybridization assays [27] and heterogeneous immunoassays[28] to only a few minutes. External magnetic fields have also been employed to increase the flux of analytes tagged with magnetic nanoparticles.[29]

Previous studies in our laboratory have demonstrated the utility of capture substrate rotation as a means to reduce the incubation time required for heterogeneous immunoassays.[30,31] In the first study, rotation was employed to increase the flux of porcine parvovirus toward the capture surface, thereby reducing assay time.[30] This study also showed that Equation 1 can be used to quantitatively account for the accumulated surface concentration (Γ_a) of the antigen as function of incubation time (t) and the concentration of antigen in the bulk solution (C_b). The first term in Equation 1 accounts for the antigen accumulation in a stagnant solution (i.e., without rotation), while the second term describes accumulation at a rotation rate of ω in a solution with a kinematic viscosity of V.

$$\Gamma_a = \frac{2}{\sqrt{\pi}} D^{1/2} C_b t^{1/2} + \frac{D^{2/3} C_b}{1.61 V^{1/6}} t \omega^{1/2} \qquad (1)$$

We also showed that this equation can serve as a basis for the determination of antigen concentration without the use of standards.[30] A second study, more closely related to the current work, reported on the use of substrate rotation to reduce the incubation time required for both antigen and label binding in a SERS sandwich immunoassay for rabbit IgG.[31] That work showed that both binding steps can be accelerated via substrate rotation, and that rotation can be effectively employed in assays in a complex biological matrix. Specifically, when compared to an assay performed under static conditions, the incubation time was reduced from 24 h to ~25 min. Interestingly, this reduction was also accompanied by a tenfold improvement in detection limit, which was due largely to a decrease in the amount of nonspecific binding.

The current paper more closely examines the effect of substrate rotation on the rate of signal development in SERS sandwich immunoassays. The main goal is to identify the origin of the improved detection limit (i.e., the reduced level of nonspecific binding) observed in our earlier report. The work reported herein therefore studied the effect of several parameters (i.e., size and concentration of the species in solution) on the rate of signal development to: (1) more fully delineate the capability of substrate rotation to speed up the binding steps in SERS sandwich assays; and (2) determine the origin of the reduced background signals.

2. Experimental

2.1. Reagents

Gold nanoparticles (60-nm diameter, 2.6 x 10^{10} particles/mL) were purchased from Ted Pella. Octadecanethiol (ODT), dithiobis(succinimidyl propionate) (DSP), 4-nitrobenzethiol (NBT), and phosphate buffered saline (PBS) packs (10 mM, pH 7.2) were obtained from Sigma-Aldrich. SuperBlock blocking buffer and BupH Borate Buffer Packs (50 mM, pH 8.5) were acquired from Pierce. Poly(dimethyl siloxane) (PDMS, Dow Corning) was used to prepare a microcontact printing stamp. Goat anti-mouse IgG polyclonal antibody was purchased from Pierce. The antibody was purified by immunoaffinity chromatography and supplied at 1.8 mg/mL in PBS (pH 7.6). Whole molecule mouse and human IgGs, also acquired from Pierce, were received at concentrations of 5.5 mg/mL and 11.0 mg/mL, respectively, in PBS (pH 7.6).

2.2. ERL preparation

The extrinsic Raman labels (ERLs) were prepared by first adjusting the pH of a 1.0-mL suspension of 60-nm gold particles to 8.5 via the addition of 40.0 µL of 50-mM borate buffer. Next, a solution containing 10.0 µL of 0.20-mM DSP (for antibody binding) in ethanol and 3.45 µL of 2.0-mM NBT (the Raman reporter molecule) in acetonitrile was added to the suspension and reacted for ~12 h to form a mixed monolayer on the gold particles. This step was followed by the addition of 20 µg of goat anti-mouse antibody (11.1 µL of 1.8 mg/mL), with the resulting suspension incubated for ~8 h.

To block any unreacted succinimidyl ester groups, 100 µL of 10% BSA in 2 mM borate buffer was added to the particle solution and reacted for ~12 h. The suspension was then centrifuged at 2000*g* for 10 min to remove excess thiols, antibody, and other residual materials. The supernatant was removed and the nanoparticles resuspended in 1.0 mL of 2 mM borate buffer containing 1% BSA. This cleanup cycle was repeated two more times. After the final rinsing step, the nanoparticles were resuspended in 0.5 mL of 1% BSA with 150 mM NaCl (to mimic physiological conditions). Finally, the suspension, which contained ~4.7 x 10^{10} particles/mL, was passed through a 0.22-µm syringe filter (Costar) to remove any large aggregates.

2.3. Capture substrate preparation

Glass microscope slides (Fisher) were cut into 1 x 1 cm squares and cleaned ultrasonically for ~30 min, first in 10% Contrad 70, then deionized water, and finally ethanol. Template stripped gold (TSG) was prepared by resistively evaporating ~250 nm of gold (99.9% purity) at a rate of ~0.2 nm/s onto a 4-in silicon [111] wafer (University Wafer) with an Edwards 306A resistive evaporator. The clean glass chips were then applied to the gold-coated wafer with two-part epoxy (Epoxy Technology) and cured at 150 °C for 1.75 h.

To prepare capture substrates, the glass chips were gently detached from the silicon wafer, which removes the sandwiched gold film, to expose a smooth gold surface. Each substrate was addressed by ~30-s exposure to an ODT-saturated PDMS stamp with a 3.0-mm hole cut in its center. The ODT forms a hydrophobic

barrier that defines a 3.0-mm sample address. The sample address was subsequently treated with a 20-µL drop of 5.0-mM DSP in dimethyl sulfoxide for 30 min to form a DSP-derived monolayer. After rinsing with ethanol and drying with high-purity nitrogen, a 20.0 µL drop of 100 µg/mL anti-mouse IgG (diluted in 50 mM borate buffer) was pipetted onto the DSP-modified address on each of the gold substrates. After allowing ~12 h for antibody coupling,[7,32,33] the substrates were rinsed with ~6 mL of 10 mM PBS. Lastly, 20.0 µL of SuperBlock buffer were placed on each capture substrate for ~12 h to block any unreacted succinimidyl groups, with the capture substrates then rinsed with 10 mM PBS.[14]

2.4. Immunoassay protocols

As mentioned, SERS assays are carried out by incubating the substrates first with the antigen solution, then with the labeling solution containing ERLs. In studies in which the kinetics of the incubation steps were not investigated, the assays were performed using our typical format (i.e., stagnant incubation of a 20-µL drop of sample or label solution for ~8-16 h). With our present hardware design, the incubations with substrate rotation required 1-mL of solution in order to fully submerge the substrate. To allow for a direct comparison, parallel stagnant incubations were performed using the same volume of solution. Specific details for each type of experiment are given in the next sections.

2.4.1. Antigen binding kinetics

The capture substrates were incubated with 1.0-mL of mouse IgG (either 10 or 100 ng/mL) for times ranging from 4 min to 8 h for stagnant incubations and from

4 min to 2 h for rotation incubations. A schematic of antigen incubation with and without rotation is presented in Figure 1a, and the specific conditions for each type of incubation are described in Section 2.5. After antigen exposure, the substrates were rinsed with 2 mM borate/150 mM NaCl (~6 mL) and exposed to 20-µL drops of ERL (9.4×10^{10} particles/mL) for ~16 h in a humidity chamber. After a final rinse with ~10 mL of 2 mM borate/150 mM NaCl, the substrates were dried under a stream of high-purity nitrogen before acquiring the Raman spectra.

2.4.2. ERL binding kinetics

The capture substrates were incubated in a quiet solution with 20-µL drops of mouse IgG (either 10 or 100 ng/mL) for ~16 h in a humidity chamber. After antigen incubation, the substrates were rinsed with 2 mM borate/150 mM NaCl (~6 mL) and exposed 1.0-mL aliquots of ERL (either 4.7×10^{10} or 9.4×10^{10} particles/mL) for times ranging from 4 min to 8 h for stagnant incubations and from 4 min to 2 h for rotation incubations (see Section 2.5). As before, the substrates were rinsed with borate/NaCl and dried with nitrogen before acquiring the Raman spectra.

2.4.3. Nonspecific binding kinetics

These procedures were identical to those used for the investigation of ERL binding kinetics, noting that the antigen incubation step was performed using 100 ng/mL human IgG. Therefore, any ERLs captured by the substrate in this experiment were the result of nonspecific binding only. Figure 1b illustrates both specific and nonspecific binding of ERL to the capture surface.

2.5. Immunoassay incubation conditions

To allow for a direct comparison between stagnant and rotation incubations, every attempt was made to ensure that rotation rate was the only variable within each set of experiments described in Section 2.4. To this end, the specific conditions for each type of incubation are given below.

2.5.1. Rotation incubations

Using double-sided tape (3M), the capture substrates were attached to the end of a rotating disk electrode (RDE) with a chemically resistant Teflon shroud, modified in-house to a diameter of 14-mm. The rod was mounted into an AFASR rotator (Pine Instrument Company) and lowered into a well (17-mm diameter) containing a 1.0-mL sample of either antigen or labeling solution and rotated at 800 rpm for varying times (from 4 min to 2 h); this rotation rate was chosen to maintain consistency with our previous rotation studies.[30,31]

2.5.2. Stagnant incubations

To mimic the conditions for rotation incubation (i.e., to minimize any other influence on signal development), the capture substrates were attached to the plungers of 3-mL polypropylene syringes (HSW) using double-sided tape and lowered into wells identical to those used for the rotation incubations. The syringe barrels were used to adjust the depth of immersion (i.e., to mimic that obtained using the rotating rod). Incubation times were varied from 4 min to 16 h.

2.6. SERS instrumentation

Raman spectra were collected with a NanoRaman I (Concurrent Analytical) fiber-optic Raman system. The excitation source is a 30-mW, 632.8-nm HeNe laser. The spectrograph consists of an f/2.0 Czerny-Turner imaging spectrometer (resolution of 6-8 cm^{-1}) and a thermoelectrically cooled (0°C) CCD (Kodak 0401E). The objective has a numerical aperture of 0.68, and focuses the laser to a 25-μm diameter spot (~3 mW) on the substrate surface. The same objective was used to collect the scattered radiation.

2.7. Data analysis

Representative SERS spectra of NBT-labeled substrates are shown in Figure 2. All of the spectral features can be assigned to the NBT label. Importantly, the intense Raman band at 1336 cm^{-1} is caused by the symmetric nitro stretch ($\nu_s(NO_2)$) of NBT. For each set of experiments, the average SERS intensity at 1336 cm^{-1}, obtained from measurements at 20 different locations on each capture surface, is plotted against incubation time for both the stagnant and rotation incubations. Figure 3 plots the predicted surface accumulation (i.e., signal development) over time for both stagnant and rotation (800 rpm) incubation in the ERLs based on Equation 1. Though not exacting, the plots are well approximated by linear regressions. Moreover, at relatively short incubation times (i.e., up to 2 h with rotation and up to 8 h without rotation), plots of the SERS signal (count/s or cps) versus incubation time (min) for both the antigen and ERL binding experiments (Sections 2.4.1 and 2.4.2) exhibited a linear relationship. Therefore, to simplify data comparison, the

slope of the linear region of each plot will be used as a measure of the signal development over time (e.g., the rate of accumulation of antigen or label at the capture surface), and is reported herein as the binding rate (cps/min) for both rotation (R) and stagnant (S) incubations. Therefore, the ratio of the slopes (R/S) for each set of plots can be viewed as an indicator of the relative increase in binding rate due to rotation.

3. Results and Discussion

3.1. Kinetics of specific binding (antigen and ERL)

As described in Section 2.4.1, the effect of rotation on the rate of binding of mouse IgG was investigated. The results from this set of experiments are plotted in Figure 4, which shows the increase in SERS signal (i.e., amount of bound antigen) with time for both 10 and 100 ng/mL mouse IgG under rotation and stagnant incubation conditions. In both cases, the rate of binding is faster under rotation conditions, but the effect is clearly more pronounced with the lower IgG concentration. In addition, increasing the antigen concentration caused the binding rates for both rotation and stagnant incubations to increase. The binding rates for each set of conditions are summarized in Table 1, along with the ratio of the binding rates with and without rotation for each of the antigen concentrations tested. These data clearly show that the effect of rotation increases with decreasing antigen concentration such that, over the concentration range tested, the antigen binding rate was increased nearly by a factor of 4 by capture substrate rotation at the lower antigen concentration.[34]

Plotted in Figure 5 are the results of the experiments described in Section 2.4.2, which investigated the effect of rotation on ERL binding. Two different concentrations of surface binding sites (corresponding to 10 and 100 ng/mL mouse IgG) and two ERL solution concentrations (4.7 and 9.4 x 10^{10} particles/mL) were tested. It is apparent from a comparison of Figures 4 and 5 that the effect of rotation is much greater with the ERLs than with the IgGs. As summarized in Table 2, rotation at 800 rpm increased the ERL binding rate by as much as ~17 times.

Drawing on the data in Tables 1 and 2, rotation clearly has a much greater effect on the rate of ERL binding than on that of antigen binding. A possible explanation for this result can be found by examining Equation 1, which predicts that the effect of rotation on flux increases with decreasing diffusion coefficient. Since the ERLs (~80 nm diameter) are much larger than the IgGs (~10 nm diameter), their diffusion coefficient is much smaller (D_{ERL} ~7x10^{-12} m^2/s vs. D_{IgG} ~4x10^{-11} m^2/s), which results in a lower rate of diffusional transport. The data in Tables 1 and 2 are consistent with this interpretation.

It is interesting to note, however, that the binding rates for the ERLs with rotation are much higher than those for the IgGs under the same conditions. Consider the binding rates reported in Table 1 for 10 ng/mL mouse IgG (~4 x 10^{10} antigens/mL) and those reported in Table 2 for the lower ERL concentration (4.2 x 10^{10} particles/mL). Though the stagnant binding rate is lower for the ERLs than the IgGs, as predicted based on diffusion coefficients, the ERL binding rate with rotation is much higher than expected, especially considering that the concentration of

surface binding sites (i.e., bound antigens) is much lower for the ERL binding experiments. This difference may indicate that the rate of antigen binding under rotation conditions is no longer diffusion limited (i.e., the kinetics of the reaction are affecting the binding rate). Since ERLs are coated with a layer of binding sites (i.e., antibodies), their rate of binding upon impact with the substrate may be much faster than that for the antigens, which are expected to have only a few binding sites. If this is the case, the probability for antigen binding is expected to be lower as the antigens may require more time than the ERLs to properly orient themselves before they can bind to the substrate.

Another important factor to examine in these binding experiments is the effect of concentration. According to Equation 1, the binding rate ($d\Gamma_a/dt$) for both rotation and stagnant incubation is directly proportional to concentration. Let us first examine the effect of concentration on the rates of antigen binding reported in Table 1. For the stagnant incubations, a 10-fold increase in concentration causes nearly a 10-fold increase in the binding rate. In the case of rotation, however, the increase in binding rate is only ~$\sqrt{10}$, which is lower than predicted. As concluded from the comparison of ERL and antigen binding rates, this result also suggests that mass transfer is a smaller contribution to the antigen binding rate under rotation conditions.

For the ERL binding experiments, we will start by examining the substrates that were exposed to 10 ng/mL antigen before ERL binding. For these substrates, the effect of rotation increases with decreasing ERL concentration, which is qualitatively consistent with the IgG binding experiments. In fact, doubling the ERL

concentration doubles the binding rate under stagnant conditions, while the binding rate under rotation conditions only increases by a factor of ~√2. This difference parallels that exhibited by the antigen binding studies, which suggests two possible explanations. First, it could be evidence that, under rotation conditions, diffusion is no longer the only factor influencing the rate of ERL binding. Another possible explanation, however, is that the binding rate is not directly proportional to concentration as predicted by Equation 1.

In the case of the substrates with a higher surface concentration of antigenic binding sites (i.e.,100 ng/mL IgG), doubling the ERL concentration increases the binding rates for both rotation and stagnant incubations by a factor of √2. In other words, the effect of rotation is weakly dependent on the concentration of the binding species (i.e., ERL) in solution. It is possible that the flux of ERLs to the surface (which depends on the ERL concentration) is not the limiting factor in the rate of ERL binding under these conditions. However, it may also be the case that an increase in flux of ~17 times is the maximum improvement possible using a rotation rate of 800 rpm. A more thorough investigation of the origins of these unexpected findings by using higher rotation rates and analyte concentrations is planned.

Another interesting aspect of Figures 4 and 5 is the step-like pattern present in several of the plots. These "steps" appear in both stagnant and rotation binding studies, and both the ERL and antigen binding curves exhibit this step-like behavior. Based on a preliminary investigation using curve-fitting techniques, we suspect that this shape is consistent with binding at a surface that contains two different types of

binding sites. For one type of binding site (i.e., Type A), the rate of surface accumulation is directly proportional to the number of available binding sites (i.e., $\Gamma_{initial} - \Gamma_a$). A plot of surface accumulation versus incubation time for this type of binding shows a linear increase to a limiting value that represents saturation of Type A sites. For a second type of binding site, (i.e., Type B), where the binding rate is directly proportional not only to the number of available binding sites, but also to the surface accumulation $[(\Gamma_{initial} - \Gamma_a)\Gamma_a]$, a plot of signal development over time has a sigmoidal shape. It follows that if both types of binding sites were present, the overall signal development could be described by the sum of the two responses, which gives a step-like shape consistent with that found in several of the plots in Figures 4 and 5. A thorough investigation of this issue will be the focus of a future publication.

3.3. Nonspecific binding kinetics

Figure 6 presents the Raman signals obtained from the nonspecific binding studies for both types of incubation (see Section 2.4.3). The results are an indication of the increase in background signal with incubation time that can be expected for assays performed using the various incubation conditions investigated in the previous experiments. As expected, the signals obtained from nonspecific binding of ERLs were much lower than those obtained for the specific binding experiments. These results also differ from those obtained for the specific antigen and ERL binding studies in that the signal development was not linear with time but instead increased with the square-root of time. This difference can be explained by examining the process of nonspecific binding of the ERL to the capture surface.

While specific interactions (i.e., antigen and ERL binding) are assumed to proceed at a rate above that of mass transport in these systems, the nonspecific binding of the ERL to the substrate is viewed as a much slower process, and is therefore not diffusion-limited. Nonspecific binding occurs because the ERL has restricted lateral diffusion in the vicinity of the capture surface, [35] which allows for the accumulation of many weak interactions (i.e., electrostatic, Van der Waals, and Lewis acid-base forces, as well as hydrophobic interactions) between the proteins on the ERL and those on the substrate. The nonspecific binding rate is therefore dependent on the rate of accumulation of these interactions, and has been found to be proportional to $\sqrt{t}$.[36] Therefore, for these experiments, the binding rates were determined from linear regressions of SERS intensity vs $t^{1/2}$.

The plots in Figure 6 clearly show that rotation has no observable effect on the rate of nonspecific binding of the ERL, an observation which is verified by the data in Table 3, which shows that the ratio of the binding rates R/S ~1. This finding is consistent with the previous assertion that the rate of nonspecific binding is not limited by mass transfer. Consequently, rotation increases the rate of specific binding (i.e., antigen and label binding) without increasing the rate of nonspecific binding (i.e., background signal development). We therefore conclude that the increase in signal-to-background ratio observed in our previous work with rotating capture substrates results from the reduced incubation time. This claim suggests that capture substrate rotation can not only decrease the time required for both incubation steps in SERS sandwich immunoassays, but will decrease the level of

nonspecific binding as a consequence, leading to shorter assays with improved limits of detection.

Examples of the improvements in signal-to-background ratios (S/B) achieved with the use of rotation for the label incubation step in this assay are given in Table 4. The labeling step is nearly 7 to 17 times faster with rotation, and the S/B ratios are a factor of 1.4 and 3.5 times higher for the samples exposed to 10 and 100 ng/mL mouse IgG, respectively. The limit of detection for each type of incubation was calculated using the standard deviation of the nonspecific background signal and the slope of a line between the background and the 10 ng/mL data point. At a rotation rate of 800 rpm, incubation in ERLs for 25 min yields a detection limit of ~0.3 ng/mL mouse IgG, while the detection limit after 8 h of stagnant incubation is ~0.5 ng/mL. Thus, the use of rotation can substantially reduce the time required for both incubations with no degradation in detection.

4. Conclusion

We have shown that the effect of substrate rotation on the rate of binding in immunoassays depends on several factors. Species with larger diffusion coefficients were less affected by rotation. Also, decreasing the concentration of the species in solution increased the effectiveness of rotation. Both relationships were predicted by Equation 1, the derivation of which was reported in our previous work with substrate rotation.[30] The results indicate that under some of the conditions tested, the binding rates may not be completely diffusion limited, and future studies are planned to more thoroughly investigate this possibility. Within the parameters tested in this study,

rotation increased the rate of specific binding events by factors ranging from ~2 to 17 times. The most significant finding of this study, however, was that rotation of the capture substrate had no effect on the rate of nonspecific binding of the label. This conclusion is important because it suggests that substrate rotation will not only shorten assay time, but may also decrease the background signal. For the data obtained herein, changing the labeling step from an 8 h quiet incubation to a 25 min incubation with rotation at 800 rpm yielded comparable limits of detection (0.5 ng/mL and 0.3 ng/mL, respectively). Future studies will focus on the effect of rotation rate on immunoassay kinetics, as well as optimizing rotation conditions for several existing SERS-based immunoassays.

Acknowledgements

The authors would like to thank Jeremy D. Driskell for many insightful discussions. This work was supported through grants from DARPA-CEROS and NIH, and by the Institute for Combinatorial Discovery of Iowa State University. The Ames Laboratory is operated for the U.S. Department of Energy by Iowa State University under contract DE-AC02-07CH11358.

References

(1) Chomel Bruno, B. *J. Vet. Med. Educ.* 2003, *30*, 145-147.

(2) Diamandis, E. P.; Christopoulos, T. K. In *Immunoassay*; Diamandis, E. P., Christopoulos, T. K., Eds.; Academic Press: San Diego, 1996, pp 1-3.

(3) Sokoll, L. J.; Chan, D. W. *Anal. Chem.* 1999, *71*, 356R-362R.

(4) White, S. R.; Chiu, N. H. L.; Christopoulos, T. K. *Methods* 2000, *22*, 24-32.

(5) Nettikadan, S. R.; Johnson, J. C.; Mosher, C.; Henderson, E. *Biochem. Biophys. Res. Commun.* 2003, *311*, 540-545.

(6) Pris, A. D.; Porter, M. D. *Langmuir* 2004, *20*, 6969-6973.

(7) Jones, V. W.; Kenseth, J. R.; Porter, M. D.; Mosher, C. L.; Henderson, E. *Anal. Chem.* 1998, *70*, 1233-1241.

(8) Kenseth, J. R.; Kwarta, K. M.; Driskell, J. D.; Porter, M. D.; Neill, J. D.; Ridpath, J. F. In *Combinatorial Materials Science*, 2007, pp 81-107.

(9) Kjeldsberg, E. *J. Virol. Methods* 1986, *14*, 321-333.

(10) Zheng, Y. Z.; Hyatt, A.; Wang, L.-F.; Eaton, B. T.; Greenfield, P. F.; Reid, S. *J. Virol. Methods* 1999, *80*, 1-9.

(11) Donaldson, K. A.; Kramer, M. F.; Lim, D. V. *Biosens. Bioelectron.* 2004, *20*, 322-327.

(12) Llic, B.; Yang, Y.; Graighead, H. G. *Appl. Phys. Lett.* 2004, *85*, 2604-2606.

(13) Driskell, J. D.; Lipert, R. J.; Porter, M. D. *J. Phys. Chem. B* 2006, *110*, 17444-17451.

(14) Driskell, J. D.; Kwarta, K. M.; Lipert, R. J.; Porter, M. D.; Neill, J. D.; Ridpath, J. F. *Anal. Chem.* 2005, *77*, 6147-6154.

(15) Grubisha, D. S.; Lipert, R. J.; Park, H.-Y.; Driskell, J.; Porter, M. D. *Anal. Chem.* 2003, *75*, 5936-5943.

(16) Park, H.-Y.; Driskell, J. D.; Kwarta, K. M.; Lipert, R. J.; Porter, M. D.; Schoen, C.; Neill, J. D.; Ridpath, J. F. *Top. Appl. Phys.* 2006, *103*, 427-446.

(17) Porter, M. D.; Driskell, J. D.; Kwarta, K. M.; Lipert, R. J.; Neill, J. D.; Ridpath, J. F. *Dev Biol (Basel)* 2006, *126*, 31-39; discussion 323.

(18) Ni, J.; Lipert, R. J.; Dawson, G. B.; Porter, M. D. *Anal. Chem.* 1999, *71*, 4903-4908.

(19) Park, H.-Y.; Lipert Robert, J.; Porter Marc, D. *Proc. SPIE* 2004, 464-477.

(20) Kneipp, K.; Kneipp, H.; Itzkan, I.; Dasari, R. R.; Feld, M. S. *J. Phys.: Condens. Matter* 2002, *14*, R597-R624.

(21) Sheehan, P. E.; Whitman, L. J. *Nano Lett.* 2005, *5*, 803-807.

(22) Myszka, D. G.; Morton, T. A.; Doyle, M. L.; Chaiken, I. M. *Biophys. Chem.* 1997, *64*, 127-137.

(23) Nygren, H.; Werthen, M.; Stenberg, M. *J. Immunol. Methods* 1987, *101*, 63-71.

(24) Stenberg, M.; Nygren, H. *J. Theor. Biol.* 1985, *113*, 589-597.

(25) Stenberg, M.; Stiblert, L.; Nygren, H. *J. Theor. Biol.* 1986, *120*, 129-140.

(26) Frackelton, A. R., Jr.; Weltman, J. K. *J. Immunol.* 1980, *124*, 2048-2054.

(27) Heller, M. J.; Forster, A. H.; Tu, E. *Electrophoresis* 2000, *21*, 157-164.

(28) Ewalt, K. L.; Haigis, R. W.; Rooney, R.; Ackley, D.; Krihak, M. *Anal. Biochem.* 2001, *289*, 162-172.

(29) Luxton, R.; Badesha, J.; Kiely, J.; Hawkins, P. *Anal. Chem.* 2004, *76*, 1715-1719.

(30) Driskell, J. D.; Kwarta, K. M.; Lipert, R. J.; Vorwald, A.; Neill, J. D.; Ridpath, J. F.; Porter, M. D. *J. Virol. Methods* 2006, *138*, 160-169.

(31) Driskell, J. D.; Uhlenkamp, J. M.; Lipert, R. J.; Porter, M. D. *Anal. Chem.* 2007, *79*, 4141-4148.

(32) Wagner, P.; Hegner, M.; Kernen, P.; Zaugg, F.; Semenza, G. *Biophys. J.* 1996, *70*, 2052-2066.

(33) Duhachek, S. D.; Kenseth, J. R.; Casale, G. P.; Small, G. J.; Porter, M. D.; Jankowiak, R. *Anal. Chem.* 2000, *72*, 3709-3716.

(34) Notably, the rate of binding for both concentrations of mouse IgG under rotation conditions is not as high as that observed in our previous report (ref. 31), which used the same concentrations of rabbit IgG. In that study, a 10 min incubation with rotation gave the same signal as a 12 h stagnant incubation. We are planning to carry out a detailed investigation of the binding kinetics of rabbit IgG to investigate this discrepancy.

(35) Wild, D.; Kusnezow, W. In *The Immunoassay Handbook, 3rd Ed.*; Wild, D., Ed.; Elsevier: New York, 2005, pp 187-189.

(36) Kusnezow, W.; Syagailo, Y. V.; Rueffer, S.; Baudenstiel, N.; Gauer, C.; Hoheisel, J. D.; Wild, D.; Goychuk, I. *Mol. Cell. Proteomics* 2006, *5*, 1681-1696.

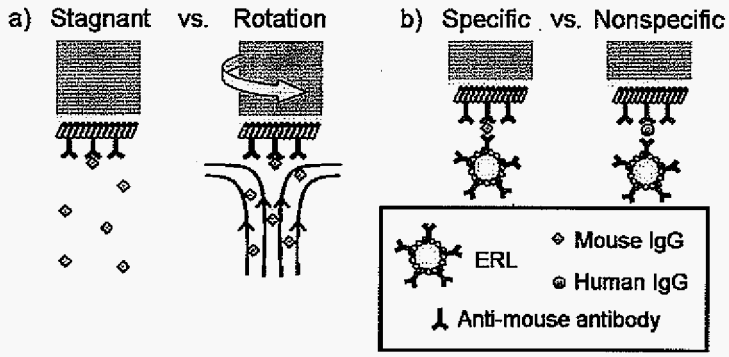

Figure 1. a) Schematic representation of antigen binding under stagnant and rotation conditions. b) Schematic representation of specific and nonspecific binding of the ERL.

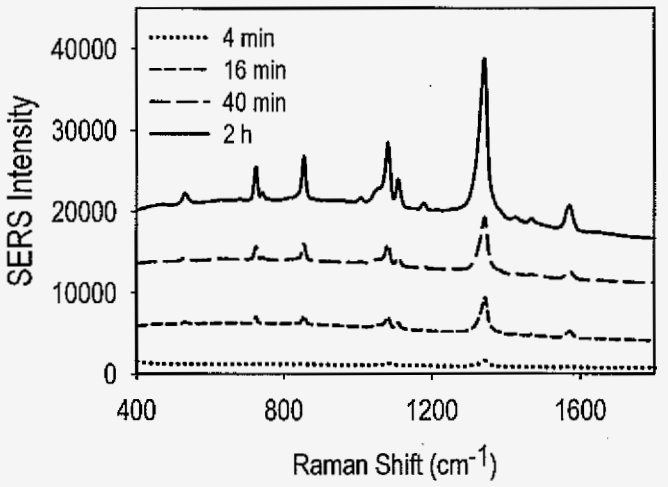

Figure 2. Representative SERS spectra of NBT-labeled substrates. After incubating for ~16 h with 20-µL drops containing 100 ng/mL mouse IgG, these substrates were labeled using an ERL solution containing 4.2×10^{10} particles/mL. The labeling step was carried out using the rotation conditions (800 rpm) described in Section 2.5.1 for the specified incubation times.

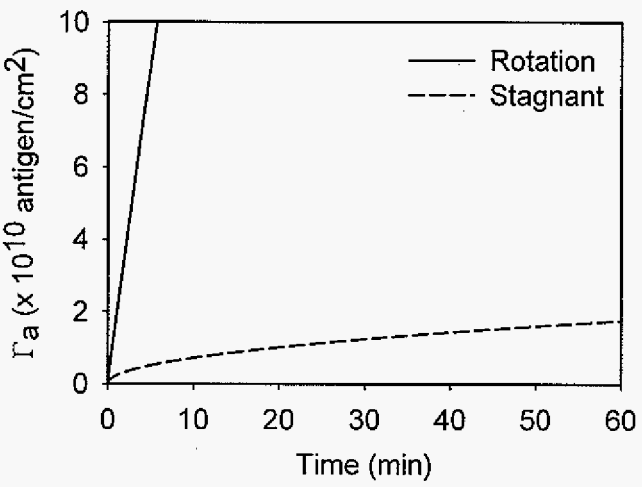

Figure 3. Illustration of predicted surface accumulation (Γ_a) over time for rotation (Equation 1) and stagnant (first term in Equation 1) incubations. The values used for concentration (4.0 x 10^{11} antigen/mL) and diffusion coefficient (4.2 x 10^{-7} cm^2/s) are the approximate experimental values for the antigen binding studies.

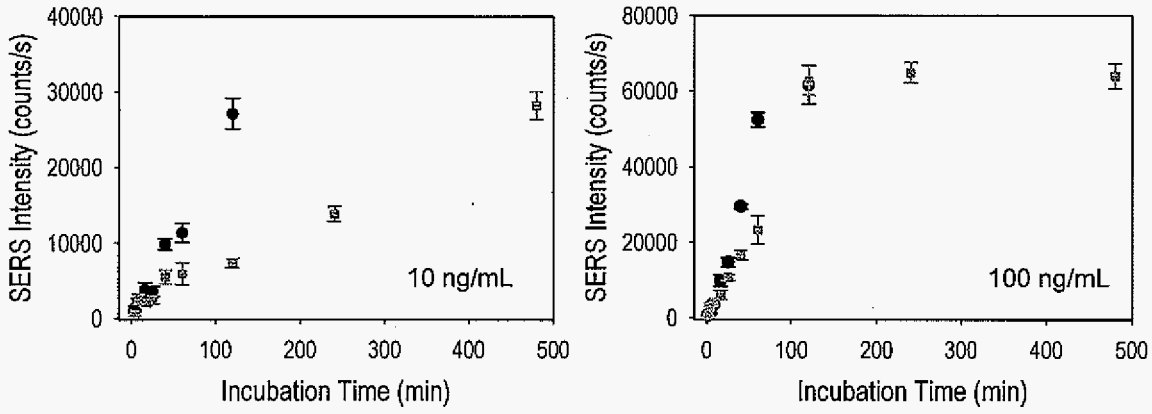

Figure 4. Plots of SERS signal intensity ($\nu_s(NO_2)$) versus incubation time for both rotation (●) and stagnant (▨) incubations in either 10 or 100 ng/mL mouse IgG. Labeling was carried out by stagnant incubation with 20-µL drops of ERL (9.4×10^{10} particles/mL) for ~16 h.

Table 1. Antigen binding rates [reported as SERS signal (counts/s or cps) over time (min)] for rotation (R) and stagnant (S) incubations calculated from the plots in Figure 4. The relative increase in binding rate is given by the ratio R/S.

[IgG] (ng/mL)	R (SERS cps/min)	S (SERS cps/min)	R/S
10	219	59.7	3.67
100	792	401	1.98

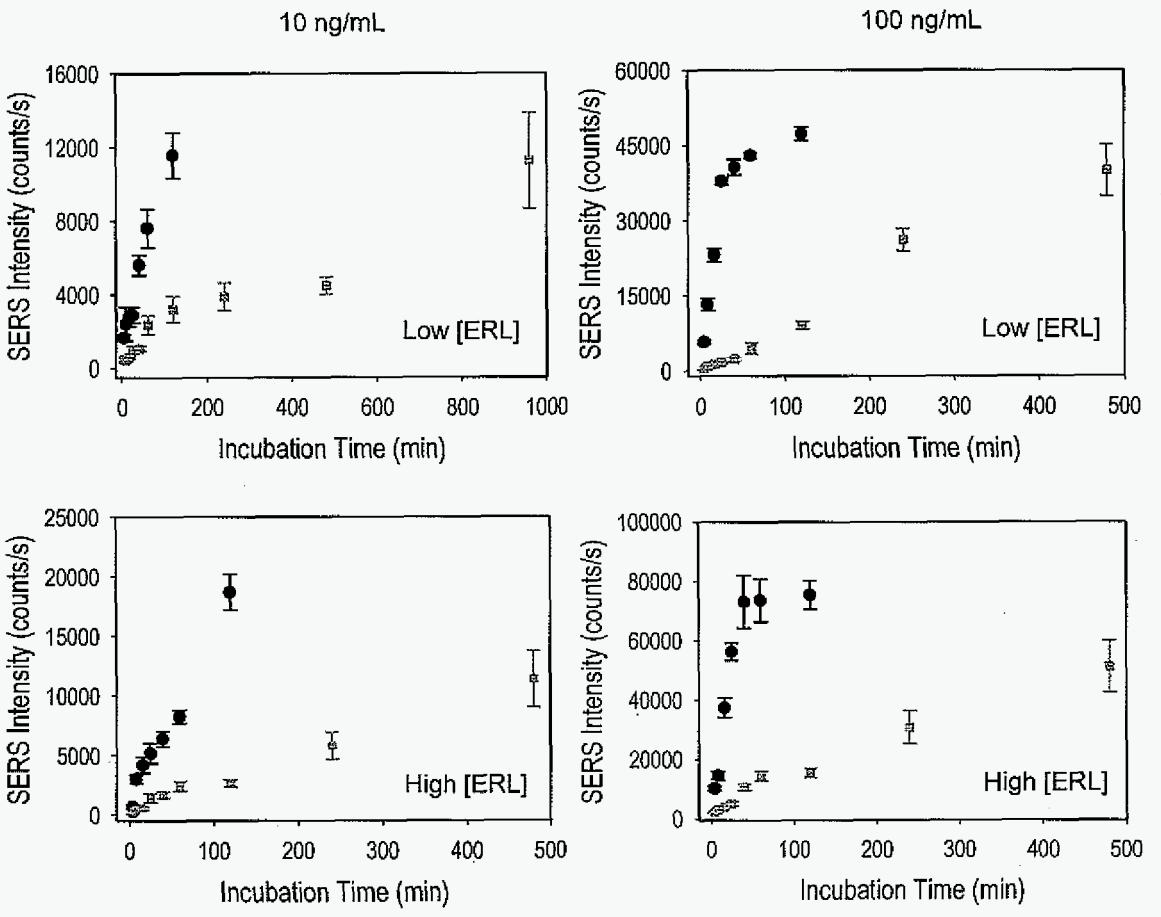

Figure 5. Plots of SERS signal intensity ($\nu_s(NO_2)$) versus incubation time for both rotation (●) and stagnant (▩) incubations in ERLs. The plots labeled "Low [ERL]" are the responses from substrates exposed to a solution containing 4.2 x 10^{10} particles/mL while those labeled "High [ERL]" used 9.4 x 10^{10} particles/mL. Before ERL exposure, substrates were incubated with stagnant, 20-µL drops of either 10 or 100 ng/mL mouse IgG for ~16 h.

Table 2. ERL binding rates [reported as SERS signal (counts/s or cps) over time (min)] for rotation (R) and stagnant (S) incubations calculated from the plots in Figure 5. The relative increase in binding rate is given by the ratio R/S.

Low ERL Concentration (4.2×10^{10} particles/mL)			
[IgG] (ng/mL)	R (SERS cps/min)	S (SERS cps/min)	R/S
10	108	11.8	9.12
100	1506	87.5	17.2
High ERL Concentration (9.4×10^{10} particles/mL)			
[IgG] (ng/mL)	R (SERS cps/min)	S (SERS cps/min)	R/S
10	158	24.0	6.59
100	1984	114	17.4

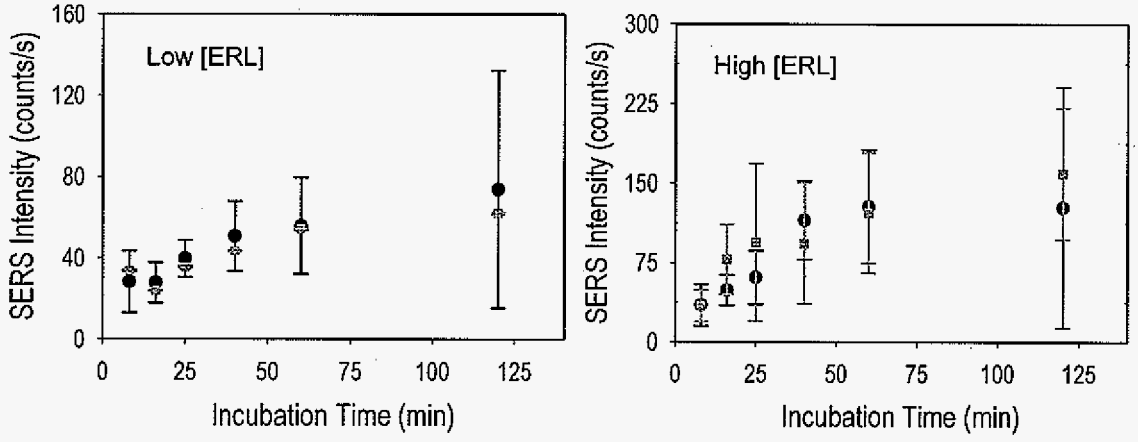

Figure 6. Plots of SERS background intensity versus incubation time for both rotation (●) and stagnant (▤) incubations in ERL. The plot labeled "Low [ERL]" is the response from substrates exposed to a solution containing 4.2 x 10^{10} particles/mL while that labeled "High [ERL]" used 9.4 x 10^{10} particles/mL. Before ERL exposure, substrates were incubated with 20-µL drops of 100 ng/mL human IgG for ~16 h.

Table 3. Nonspecific binding rates [reported as SERS signal (counts/s or cps) over sqrt. time ($min^{1/2}$)] for rotation (R) and stagnant (S) incubations calculated from the plots in Figure 6. The relative increase in binding rate is given by the ratio R/S.

[ERL] (particles/mL)	R (SERS cps/$min^{1/2}$)	S (SERS cps/$min^{1/2}$)	R/S
4.2×10^{10}	7.26	6.47	1.08
9.4×10^{10}	13.8	15.4	0.896

Table 4. Comparison of signal-to-background ratios (S/B) obtained from ERL incubations under both stagnant and rotation conditions. The nonspecific binding signals were obtained from the data plotted in Figure 6 while the signals for the substrates containing bound mouse IgG (i.e., specific binding) were taken from the data plotted in Figure 5.[a]

	Nonspecific Binding	10 ng/mL Mouse IgG		100 ng/mL Mouse IgG	
Incubation Conditions	Background Intensity (cps)	SERS Intensity (cps)	S/B	SERS Intensity (cps)	S/B
25 min Rotation	61.0	5180	84.9	56256	922
8 h Stagnant	193	11373	58.9	51151	265

a. Values are from substrates labeled with an ERL concentration of 9.4×10^{10} particles/mL.

GENERAL CONCLUSIONS AND FUTURE PROSPECTUS

The main focus of this dissertation is the development of C-SPE technology for monitoring water quality during spaceflight. Along with previous work in our laboratory, the results presented herein have proven that C-SPE is a versatile technique capable of determining in microgravity the concentration of a wide range of analytes that affect spacecraft water quality. Chapters 2 and 3 described the expansion of C-SPE technology to the detection of two new analytes, i.e., colloidal silver and formaldehyde. Moreover, the analyses of silver(I) and total silver discussed in Chapter 2 demonstrate that C-SPE analyses can provide information on analyte speciation as well as concentration. The applicability of C-SPE was expanded to include organic analytes by the development of a method for determining formaldehyde, as detailed in Chapter 3. Furthermore, efforts are under way to extend this approach to determinations of glycols, a high priority organic analyte for NASA water quality monitoring applications, by simply adding an oxidizing agent to the existing formaldehyde method.

The development of C-SPE as a water quality monitoring technology for spaceflight applications entails not only providing techniques that span NASA's list of critical water quality parameters, but also ensuring that the techniques will function under the conditions associated with spaceflight. According to recent microgravity testing of C-SPE methods and procedures, presented in Chapter 1, C-SPE technology is capable of functioning in a weightless environment. Previous experiments had proven only that the C-SPE analyses of silver and iodine could be

accomplished in microgravity using samples that were collected into syringes and de-bubbled under normal gravity conditions.[1,2] However, spaceflight deployment of this technology will require the collection and metering of accurate sample volumes under microgravity conditions. To this end, the flight results reported in Chapter 1 proved that it is possible to collect a target volume of bubble-free water in microgravity using fairly simple manual manipulation techniques. Moreover, excellent agreement between ground and flight data was achieved for the C-SPE analyses of silver(I) and iodine (I_2) where the entire experimental process (i.e., from sample collection to data acquisition) for the flight analyses was performed in microgravity.

Also reported in Chapter 1 were the results from microgravity tests of the feasibility of collecting a bubble-free water sample in a syringe via a cartridge used to introduce reagents into the sample. The flight results proved that, using simple manual manipulation techniques, 1.0-mL and 10.0-mL samples of bubble-free water could be collected into 3-mL and 10-mL syringes despite the introduction of nearly 2 mL of air from the cartridge. The insights gained in this flight experiment were used in a recent evaluation of the C-SPE method for total iodine in microgravity. The experimental procedure for the total iodine method, including the collection of a bubble-free 10.0-mL sample via a reagent cartridge, was successfully performed in microgravity (i.e., flight and ground results showed excellent agreement). The same flight results will be useful in the future microgravity validation of the total silver and formaldehyde methods, both of which, as described in Chapters 2 and 3, require collecting a 1.0-mL sample in a 3-mL syringe. Though experience has proven that

unexpected challenges can arise when testing a new experimental procedure in microgravity, our success in overcoming the challenges we have encountered thus far gives us no reason to doubt the continued development of spaceflight-compatible C-SPE methods.

Though C-SPE has been proven to be a viable option for spaceflight deployment, there are still a few areas where improvements to the technology could greatly increase its usefulness for space exploration. While the analyses developed thus far require only ~2 min to complete, the time required to determine multiple analytes can be significant. Though water quality monitoring is vital to crew health, the majority of astronaut time should ideally be focused on accomplishing mission objectives rather than on water testing. We are therefore developing a multiplexed analysis system that could increase the number of water quality parameters tested without increasing the investment of crew time.

The scope of C-SPE technology extends beyond spaceflight with numerous Earth-bound applications. Because C-SPE allows for analyte quantification on-membrane, thereby eliminating the need for elution with organic solvents, C-SPE is an environmentally friendly and cost effective alternative to existing SPE-based techniques. Moreover, several C-SPE techniques, including the total silver and formaldehyde methods presented herein, have proven to be superior to commercially-available water testing kits for determining the same analyte. However, the applicability of C-SPE technology is not limited to water quality testing. In fact, C-SPE could be applied to the detection of numerous analytes of interest in fields

ranging from environmental monitoring to homeland security. In addition, C-SPE techniques could be adapted to the analysis of samples other than water, which could expand the utility of the technology to fields such as forensic toxicology, where C-SPE could be used to detect drugs in body fluids. These and other avenues are currently being explored in our laboratory.

References

(1) Porter, M.; Arena, M.; Weisshaar, D.; Mudgett, P.; Rutz, J.; Benoit, M.; Colorimetric Solid Phase Extraction Measurements of Spacecraft Drinking Water Contaminants in: *KC-135 Postflight Report*, 2004.

(2) Porter, M. D.; McCoy, J. T.; Hazen-Bosveld, A. A.; Lipert, R. J.; Nordling, J.; Shih, C. J.; Gazda, D. B.; Rutz, J.; Straub, J.; Schultz, J.; Alverson, J.; Colorimetric Solid Phase Extraction Measurements of Spacecraft Drinking Water Contaminants in: *C-9 Postflight Report*, 2006.